Chinese Journal of Structural Chemistry

REVIEW

Recent Advances of Cu-Based Materials for Electrochemical Nitrate Reduction to Ammonia

Tianlun Ren[1], Youwei Sheng[1], Mingzhen Wang[1], Kaili Ren[1], Lianlian Wang[2]* and You Xu[1]*

[1]*State Key Laboratory Breeding Base of Green-Chemical Synthesis Technology, College of Chemical Engineering, Zhejiang University of Technology, Hangzhou 310014, P. R. China*

[2]*Department of Chemistry, Baotou Teachers' College, Baotou 014030, P. R. China*

ABSTRACT The pollution of nitrate in groundwater has become an environmental problem of general concern due to adverse human and ecological impacts. Treatment of nitrate-rich wastewater is of significance yet challenging for the conventional biological denitrification processes. Electrocatalytic nitrate-to-ammonia conversion emerges as one of the most promising avenues to remove environmentally harmful nitrate from various types of wastewaters while simultaneously producing value-added ammonia. Cu-based materials show great advantages in promoting selective electroreduction of nitrate to ammonia in terms of high nitrate conversion efficiency, ammonia selectivity and ammonia faradaic efficiency thanks to the 3d transition metal structure, low cost, high reserves, and excellent catalytic performance of Cu. In this review, we comprehensively overview the most recent advances in selective electrocatalytic nitrate-to-ammonia conversion using Cu-based materials. Various kinds of Cu-based materials including monometallic Cu catalysts, bimetallic Cu-based catalysts, Cu-based compounds, and Cu-based inorganic-organic hybrid materials and their derivatives are discussed in detail with emphasis on their structural and compositional features and functional mechanisms in promoting nitrate-to-ammonia conversion. Finally, a brief discussion on future directions, challenges and opportunities in this field is also provided.

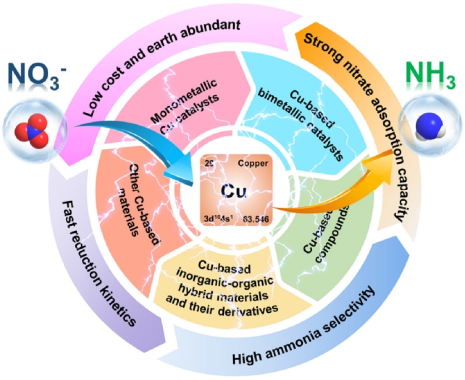

Keywords: copper, nitrate reduction reaction, ammonia synthesis, electrocatalytic, catalyst design

n INTRODUNTION

Ammonia (NH_3) is considered as a promising energy carrier, which is expected to play a resilient and sustainable role in future energy scenarios.[1] Meanwhile, NH_3 holds a main component in nitrogen fertilizers and the chemical industry.[2-5] Currently, the industrial synthesis of ammonia still relies on the Haber-Bosch process operating at high temperature and pressure conditions, which results in a large amount of fossil fuel consumption and greenhouse gas emissions (Figure 1).[6-9] Recently, electrocatalytic nitrogen reduction reaction (NRR) has been recognized as a promising way to produce ammonia, benefiting from the fact that the conversion of N_2 to NH_3 is achieved via using water as a hydrogen source and renewable electricity as energy source under ambient conditions.[10-14] However, the low NH_3 yield rate and Faradaic Efficiency (FE), due to the low aqueous solubility of N_2, the strong N≡N bond energy (941 kJ mol^{-1}) of inert N_2 and the competitive hydrogen evolution reaction (HER), seriously hinder the development and application of the NRR technology.[15-19] Therefore, it is attractive to explore more efficient, sustainable and scalable water-soluble nitrogen sources for the industrial-scale electrosynthesis of ammonia.

Among various nitrogen sources, nitrate (NO_3^-) exhibits extremely high solubility in aqueous electrolytes, which is beneficial for the adsorption and activation of nitrate on the electrode surface. Meanwhile, as the highest oxidized form of nitrogen, nitrate is widely distributed in the living environment.[20-23] On one hand, the discharge of industrial wastewater, the overuse of nitrogen-containing agricultural fertilizers and the improper disposal of animal manure lead to high nitrate nitrogen levels in surface and groundwater, which threaten aquatic ecosystems and human health.[24-26] Various nitrate treatment processes have been developed to eliminate the pollution of water resources caused by nitrate, such as reverse osmosis, ion exchange, biological denitrification and electrodialysis.[27-31] However, these processes may have the risk of causing secondary pollution or inducing pathogenic bacteria, and only involve the collection and enrichment of nitrate.[32-34] The electrochemical nitrate reduction reaction (NO_3RR) is an emerging technology for nitrate treatment, which could potentially produce high value-added product NH_3 by rationally controlling reaction conditions.[35-38] On the other hand, nitrogen oxides (NO, NO_2, etc.) in exhaust gases from fossil fuel combustion (e.g., power plants, chemical plants, and motor vehicles) cause a range of environmental and health problems.[39,40] The traditional NO_x treatment process is to convert NO_x to harmless N_2 by selective noncatalytic reduction (SNCR) and selective catalytic reduction (SCR).[41-42] However, these technologies face the disadvantages of high temperature, high operating costs and continuous supply of reducing agent. Notably, NO_x can be converted into nitrate solution by oxidation and leaching absorption.[43,44] The obtained nitrate solution could be further electrochemically reduced to high value-added ammonia. Moreover, thermodynamically, unlike the NRR process, the NO_3RR process requires lower energy to

DOI: 10.14102/j.cnki.0254-5861.2022-0201

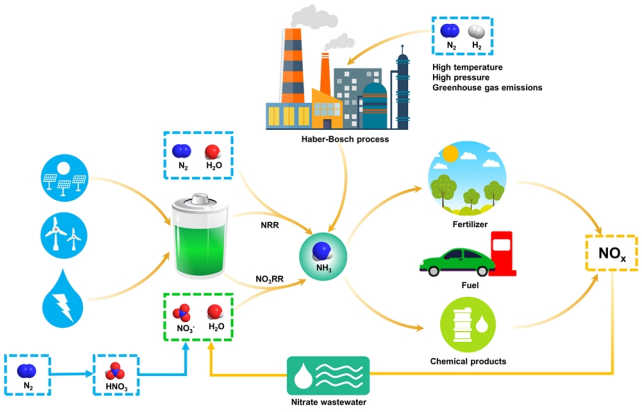

Figure 1. Schematic illustration of sustainable ammonia synthesis via nitrate electrochemical reduction.

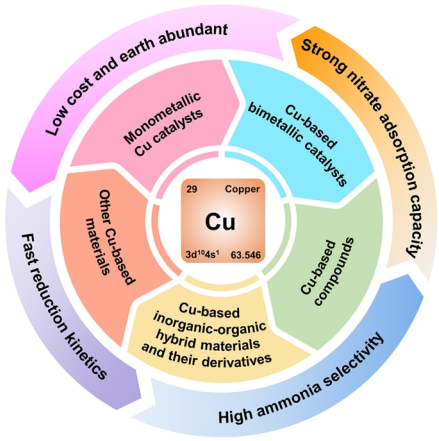

Figure 2. Schematic illustration of the advantages of Cu-based materials for nitrate reduction to ammonia.

break the N=O bond (204 kJ mol^{-1}) in nitrate.[45,46] Therefore, the waste-to-energy technology, which utilizes NO_3^- in wastewater or NO_x in exhaust gas as nitrogen sources to produce NH_3 via the NO_3RR process, is meaningful.

In the electrochemical reduction of nitrate to ammonia, the actual potential of NO_3^- to NH_3 is usually more negative than the HER potential (0 V versus reversible hydrogen electrode, RHE), thereby inevitably causing HER.[17,47,48] The conversion from high-valence NO_3^- to low-valence NH_3 is a complex process involving an eight-electron transfer process ($NO_3^- + 9H^+ + 8e^- \rightarrow NH_3 + 3H_2O$).[49,50] During the process, various undesirable by-products (such as N_2, NO_2^-, N_2O, etc.) may be formed, and thus inhibit the formation of target product ammonia.[51,52] Therefore, the investigation of suitable electrocatalytic materials to improve the FE and selectivity of ammonia is an important research topic in the electrochemical ammonia synthesis from nitrate. In recent years, a considerable number of metal catalysts (including Ru, Ir, Pd, Pt, Ni, Co, Cu, Fe and so on) and their related compounds have been applied as electrocatalysts for the selective conversion of nitrate to ammonia.[17,36,46,49,53-57]

Among these potential catalysts, Cu-based materials are undoubtedly one of the most effective electrocatalysts for the conversion of NO_3^- to NH_3 (Figure 2). On one hand, from the perspective of economy, although some noble metal catalysts exhibit high activity and ammonia selectivity in the NO_3RR process, their practical application is hampered by the scarcity and high cost.[58] The low-cost and earth-abundant Cu-based materials are more suitable for practical production applications.[59] On the other hand, from the perspective of reaction dynamics, compared with other metal catalysts, Cu-based materials have stronger catalytic capacity for nitrate reduction to ammonia. Not only does Cu have a strong adsorption capacity for nitrate, but it exhibits fast reduction kinetics in the rate-determining step of the reduction of $*NO_3$ to $*NO_2$.[32,60-62] In fact, benefiting from these excellent properties, Cu-based catalysts have received extensive attention as electrocatalysts for nitrate reduction to ammonia. A large number of Cu-based catalysts have demonstrated remarkable catalytic performance.

The past decades have witnessed the vigorous development of electrochemical NO_3RR technology, and a large amount of scientific and technical knowledge has been accumulated and some review articles on electrocatalytic NO_3RR have been published. For example, Zhang et al. reviewed the latest development of non-noble metal electrocatalysts for nitrate reduction.[32] Nirala Singh and his coworkers summarized the recent discoveries in the reaction mechanism of heterogeneous electrocatalytic NO_3RR.[63] In view that many new breakthroughs in the study of properties and structures of NO_3RR electrocatalysts have been achieved and the applications are fruitful, our intention is to provide timely updates, with particular emphasis on Cu-based catalysts. In this review, we mainly focus on the latest development of Cu-based catalysts for electrochemical nitrate reduction to ammonia. Different types of Cu-based materials that can be used for electrocatalytic NO_3RR for ammonia synthesis, involving monometallic Cu catalysts, bimetallic Cu-based catalysts, Cu-based compounds, and Cu-based inorganic-organic hybrid materials and their derivatives, are discussed in detail. The structural characteristics and catalytic mechanism of various Cu-based catalyst systems are discussed, with special emphasis on several important and representative examples. In the end section, current issues of Cu-based catalysts are briefly discussed and a vision of future challenges and opportunities is provided.

n FUNDAMENTAL MECHANISM OF NO_3RR OVER COPPER-BASED ELECTROCATALYSTS

The electrochemical reduction of nitrate to ammonia, involving a series of reaction intermediates and pathways, is a complex eight electron transfer and nine proton process.[64,65] Therefore, it is meaningful to investigate and discuss the electroreduction mechanism of nitrogen from high-valent nitrate to low-valent ammonia. The NO_3RR process includes two different reduction mechanisms. One is the adsorbed active atomic hydrogen-mediated ($H_{(ads)}$) reduction pathway, which is obtained from the reduction of protons by cathode electrons (Volmer process, Eq. (1)).[32,66] The other is performed by electron transfer and H^+.[67] As shown in Figure 3, both mechanisms begin with the

DOI: 10.14102/j.cnki.0254-5861.2022-0201

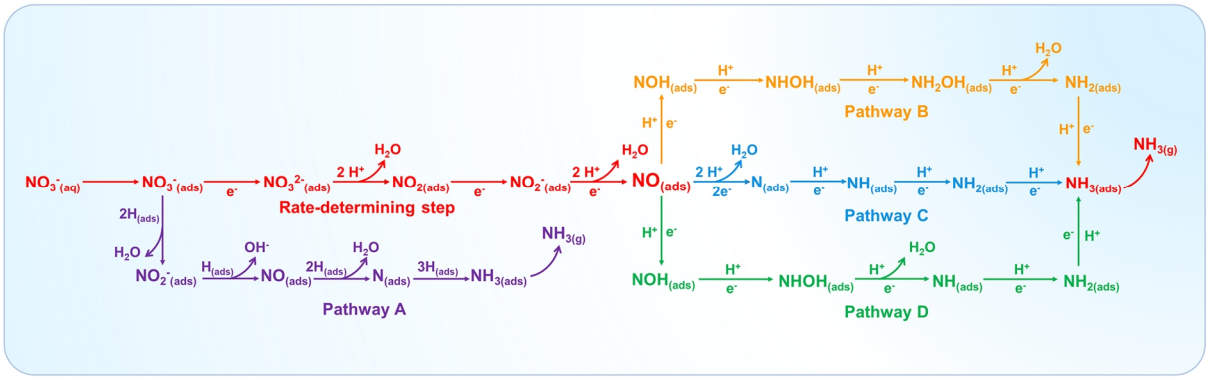

Figure 3. Schematic presentation of possible mechanism for electrochemical nitrate reduction to ammonia.

adsorption of nitrate in solution on the catalyst surface via two oxygen atoms in a chelating O,O-bidentate configuration.[63] The NO_3RR mechanism is different for various Cu-based catalysts. For composite catalysts are prepared by Cu and other metals with high affinity for adsorbing active atomic hydrogen (such as Pt, Ni, Rh, etc.), it is more likely to perform via the atomic hydrogen-mediated reduction mechanism (Pathway A).[67,68] In this pathway, atomic $H_{(ads)}$, as a strong reducing agent, can be deoxidized step by step from nitrate adsorbed on the catalyst surface ($NO_3^-{}_{(abs)}$) to form $N_{(abs)}$ (Eq. (2)-(4)), and then the formed $N_{(abs)}$ is hydrogenated and desorbed to obtain ammonia (Eq. (5)-(7)).[69,70] The reaction between the atomic $H_{(ads)}$ and $NO_3^-{}_{(abs)}$ is considered as the rate-determining step in the atomic $H_{(ads)}$ mediated NO_3RR process.[30] Notably, the atomic $H_{(ads)}$ reduction pathway may inhibit the occurrence of some side reactions since it is usually performed in a low overpotential range. Furthermore, the $H_{(ads)}$ migration barrier of 0.10 eV is lower compared to the migration barrier of $N_{(ads)}$ (0.75 eV), and the formation of N-H bond is kinetically easier than that of the N-N bond.[67,71] Thus, the enhanced affinity of the Cu-based catalyst surface for atomic $H_{(ads)}$ facilitates the ammonia production.

$$H_2O + e^- \rightarrow H_{(ads)} + OH^- \quad (1)$$
$$NO_{3(abs)}^- + 2H_{(ads)} \rightarrow NO_{2(ads)}^- + H_2O \quad (2)$$
$$NO_{2(ads)}^- + H_{(ads)} \rightarrow NO_{(abs)} + OH^- \quad (3)$$
$$NO_{(abs)} + 2H_{(ads)} \rightarrow N_{(abs)} + H_2O \quad (4)$$
$$N_{(abs)} + H_{(ads)} \rightarrow NH_{(abs)} \quad (5)$$
$$NH_{(abs)} + H_{(ads)} \rightarrow NH_{2(abs)} \quad (6)$$
$$NH_{2(abs)} + H_{(ads)} \rightarrow NH_{3(abs)} \quad (7)$$

As for the electron transfer pathway, it is more likely to occur on monometallic copper and Cu-based catalysts with low affinity for atomic $H_{(ads)}$ due to their strong adsorption capacity for nitrate. In the electron transfer mechanism, the reduction of $NO_3^-{}_{(abs)}$ to $NO_2^-{}_{(abs)}$, in which electrons are difficult to transfer into the π* orbital due to the lowest unoccupied molecular π* orbital (LUMO π*) of NO_3^-, has been noted as the rate-determining step.[70,72] For Cu-based catalysts, the d-orbital energy level is similar to the LUMO π* of NO_3^-, which is beneficial for charge injection into the LUMO π* of NO_3^- by promoting electron transfer.[73,74] The conversion from $NO_3^-{}_{(abs)}$ to $NO_2^-{}_{(abs)}$ is usually achieved via an electrochemical-chemical-electrochemical pathway. Specifically, $NO_3^-{}_{(abs)}$ is first electrochemically converted to short-lived $NO_3^{2-}{}_{(abs)}$ (Eq. (8)). Then, the $NO_3^{2-}{}_{(abs)}$ reacts chemically with 2 H^+ to form $NO_{2(abs)}$ (Eq. (9)). $NO_2^-{}_{(abs)}$ is finally obtained by a second electron transfer process (Eq. (10)). The electron transfer and hydrolysis reactions further occur on $NO_2^-{}_{(abs)}$ to form $NO_{(abs)}$, as shown in Eq. (11).[66,75,76] As the divergent center, the adsorption energies of $NO_{(abs)}$ on the Cu-based catalysts surface and the reaction environment play a key role in determining the product selectivity. The various parallel reduction pathways of $NO_{(abs)}$ will lead to a series of products, such as NH_3, N_2, NO_2 and so on.[71,73]

$$NO_{3(abs)}^- + e^- \rightarrow NO_{3(abs)}^{2-} \quad (8)$$
$$NO_{3(abs)}^{2-} + 2H^+ \rightarrow NO_{2(ads)} + H_2O \quad (9)$$
$$NO_{2(ads)} + e^- \rightarrow NO_{2(abs)}^- \quad (10)$$
$$NO_{2(abs)}^- + 2H^+ + e^- \rightarrow NO_{(abs)} + H_2O \quad (11)$$

The electrochemical-electrochemical pathways are implemented for the conversion from $NO_{(abs)}$ to NH_3, which can be divided into three possible pathways depending on the sequence of deoxygenation and hydrogenation. Regarding Pathway B, the $NH_2OH_{(abs)}$ is first formed by the stepwise hydrogenation of $NO_{(abs)} \rightarrow NOH_{(abs)} \rightarrow NH_2OH_{(abs)}$, and then $NH_2OH_{(abs)}$ undergoes deoxygenation and hydrogenation reactions to produce $NH_{3(abs)}$ (Eq. (12)-(16)).[17,75,77] Notably, the $NH_2OH_{(abs)}$ intermediates are easily desorbed from the catalyst surface to produce byproduct hydroxylamine. There are reports that the byproduct hydroxylamine is detected in the NO_3RR process catalyzed by various Cu-based catalysts, and these results confirm the existence of Pathway B.[61] In Pathway C, $NO_{(abs)}$ is directly deoxygenated by electrons and H^+ to generate $N_{(ads)}$, followed by step-by-step electrocatalytic hydrogenation to $NH_{3(abs)}$ (Eq. (17)-(20)).[78-80] Recently, Gua et al. reported a new electrochemical reduction pathway from nitrate to ammonia (Pathway D).[81] Similar to Pathway B, $NHOH_{(abs)}$ is obtained via a two-step hydrogenation reaction of $NO_{(abs)}$. The difference is that $NHOH_{(abs)}$ is directly deoxygenated to $NH_{(abs)}$ (Eq. (21)) and then hydrogenated to $NH_{3(abs)}$ along the same path as Pathway C. The density functional theory (DFT) calculations indicate that the conversion from $NO_{(abs)}$ to $NOH_{(abs)}$ requires a low activation energy of 0.08 eV on Cu (111), which is much smaller than that of $NO_{(abs)}$ to $N_{(abs)}$ (1.62 eV), although Pathway C is energetically more beneficial than Pathway B and D for thermodynamics. Furthermore, a lower activation energy is required from $NHOH_{(abs)}$

DOI: 10.14102/j.cnki.0254-5861.2022-0201

Tables 1. Performance of Cu-based Electrocatalysts for the Reduction of Nitrate to Ammonia under Neutral and Acidic Conditions.

electrocatalysts	electrolytes	NH_3 yield rate	FE (%)	potentials	ref.
CuPc@MXene	0.5 M Na_2SO_4, 50 mg L^{-1} NO_3^--N	0.72 mg h^{-1} cm^{-2}	—	-1.06 V vs. RHE	[62]
Cu@CuHHTP	0.5 M Na_2SO_4, 500 mg L^{-1} NO_3^-	1.84 mg h^{-1} cm^{-2}	67.55	-0.90 V vs. RHE	[82]
$La_2Cu_{0.8}Co_{0.2}O_4$	0.5 M Na_2SO_4, 50 mg L^{-1} nitrate	0.0699 mmol h^{-1} mg^{-1}	—	-0.68 V vs. RHE	[83]
Cu@C-800	0.1 M Na_2SO_4, 500 mg L^{-1} NO_3^-	51.7 ± 0.6 mmol h^{-1} g^{-1}	78 ± 0.9	-0.9 V vs. RHE	[84]
1-Cu'	0.5 M Na_2SO_4, 5 mM $NaNO_3$	53.43 mg_{NH3} h^{-1} mg_{Cu}^{-1}	85.5	-0.9 V vs. RHE	[85]
TiO_2 NTs/CuO_x	0.5 M Na_2SO_4, 100 mg L^{-1} KNO_3-N	264.4 mmol g^{-1} h^{-1}	83.51	-0.85 V vs. RHE	[86]
SCF	0.5 M Na_2SO_4, 100 mg L^{-1} KNO_3-N	0.31 mmol h^{-1} cm^{-2}	70	-1.3 V vs. RHE	[87]
Ni_1Cu-SAA	0.5 M K_2SO_4, 200 mg L^{-1} NO_3^--N	326.7 μmol h^{-1} cm^{-2}	~100	-0.55 V vs. RHE	[88]
plasma treated Cu_2O	0.5 M Na_2SO_4, 50 mg L^{-1} $NaNO_3$-N	0.083 mmol h^{-1} mg^{-1}	89.5	-0.58 V vs. RHE	[89]
CuNi/NC-51	0.05M Na_2SO_4, 50 mg L^{-1} NO_3^-	—	79.6	-1.0 V vs. Ag/AgCl	[90]
Rh@Cu-0.6%	0.1 M Na_2SO_4, 0.1 M KNO_3	—	93	-0.2 V vs. RHE	[91]
Ag/Cu_2O	0.5 M Na_2SO_4, 100 mg L^{-1} nitrate-N	—	96.45	-0.80 V vs. RHE	[92]
island-like Cu	0.5 M Na_2SO_4, 50 mM KNO_3	—	98.28	-0.8 V vs. RHE	[93]
$Cu_{52}Al_{48}$-LDO-r	50 mM Na_2SO_4, 22.5 mg L^{-1} NO_3^--N	661.6 mg-N m^{-2} h^{-1}	70.4	-1.10 V vs. Ag/AgCl	[94]
Cu NDs	0.01 M $NaNO_3$	500 μg $h^{-1}cm^{-2}$	97	-0.3 V vs. RHE	[95]
THH Cu NCs	100 mM K_2SO_4, 100 mM KNO_3	9.13 mmol h^{-1} cm^{-2}	98.3	-0.90 V vs. RHE	[96]
FOSP-Cu-0.1	0.5 M Na_2SO_4, 0.1 M KNO_3	101.4 μmol h^{-1} cm^{-2}	93.91	-0.266 V vs. RHE	[97]
PdCu/Cu_2O	0.5 M Na_2SO_4, 100 mg L^{-1} NO_3^--N	0.190 mmol h^{-1} cm^{-2}	94.32	-0.80 V vs. RHE	[44]
Cu/Cu_2O NWAs	0.5 M Na_2SO_4, 200 mg L^{-1} NO_3^--N	0.2449 mmol h^{-1} cm^{-2}	95.8	-0.85 V vs. RHE	[98]
Cu/Pd/CuO_x	0.5 M K_2SO_4, 50 mg L^{-1} NO_3^--N	1510.33 μg h^{-1} mg^{-1}	84.04	-1.3 V vs. SCE	[99]
Cu@$Cu_{2+1}O$ NWs	0.5 M K_2SO_4, 50 mg L^{-1} NO_3^--N	576.53 μg h^{-1} mg^{-1}	87.07	-1.2 V vs. SCE	[100]
CuO@MnO_2/CF	0.5 M K_2SO_4, 200 mg L^{-1} KNO_3-N	0.240 mmol h^{-1} cm^{-2}	94.92	-1.3 V vs. SCE	[101]
CuPd/CN	0.5 M K_2SO_4, 200 mg L^{-1} KNO_3-N	0.0904 mmol h^{-1} $mg^{-1}_{cat.}$	96.16	-1.1 V vs. SCE	[102]
dr-Cu NPs	0.5 M K_2SO_4, 50 mg L^{-1} KNO_3-N	781.25 μg h^{-1} mg^{-1}	85.47	-1.3 V vs. SCE	[103]
CuPd aerogels	0.5 M K_2SO_4, 50 mg L^{-1} KNO_3-N	784.37μg h^{-1} mg^{-1}	90.02	-0.46 V vs. RHE	[104]
Cu_3Fe	0.1 M Na_2SO_4 and 100 mg L^{-1} NO_3^-	—	74.2	-0.7 V vs. RHE	[105]
PPy-Cu-E	0.4 M K_2SO_4, 0.2 M KNO_3	0.588 mmol mg_{cat} h^{-1}	91.95 ± 1	-0.61 V vs. RHE	[106]
Pd-Cu_2O CEO	0.5 M K_2SO_4, 50 mg L^{-1} KNO_3-N	925.11 μg h^{-1} $mg_{cat.}^{-1}$	96.56	-1.3 V vs. SCE	[107]
Mo/H-CuW	0.5 M Na_2SO_4, 0.05 M NO_3^-	5.84 mg h^{-1} $mg_{cat.}^{-1}$	94.60	-0.7 V vs. RHE	[108]
Cu-Co_3O_4	0.1 M Na_2SO_4, 500 mg L^{-1} NO_3^-	36.71 mmol h^{-1} g^{-1}	86.5	-0.6 V vs. RHE	[109]
$CuCo_2O_4$	0.1 M Na_2SO_4, 1.0 mM KNO_3	48.8 μg h^{-1} cm^{-2}	34.2	-0.85 V, -0.45 V vs. RHE	[110]
Cu-N-C	0.05 M Na_2SO_4, 50 mg L^{-1} NO_3^-	37 μg h^{-1} cm^{-2}	—	-1.3 V vs. SCE	[111]
Cu-PTCDA	0.1 M PBS, 500 mg L^{-1} NO_3^-	436 ± 85 μg h^{-1} cm^{-2}	85.9	-0.4 V vs. RHE	[47]
$Cu_{2.5}Co$	0.5 M Na_2SO_4, 0.1 M KNO_3	164.23 mmol h^{-1} cm^{-2}	95.43	-0.25 V vs. RHE	[112]
CuO@$CuFe_2O_4$	0.1 M PBS, 0.1 M KNO_3	9.21 mg h^{-1} $mg_{cat.}^{-1}$	91.08	-1.0 V vs. RHE	[113]
Cu-N-C	0.5 M Na_2SO_4, 50 mg L^{-1} NO^-_3-N	9.23 mg h^{-1} $mg^{-1}_{cat.}$	—	-1.5 V vs. SCE	[114]
Cu/CuOx/CF	0.5 M K_2SO_4, 200 mg L^{-1} NO_3^--N	0.21 mmol h^{-1} cm^{-2}	93.58	-1.3 V vs. SCE	[115]
CuO@PANI/CF	0.5 M K_2SO_4, 200 mg L^{-1} KNO_3-N	0.213 mmol h^{-1} cm^{-2}	93.88	-1.3 V vs. SCE	[116]
arCu/Ni	0.1 M Na_2SO_4, 45 mg L^{-1} KNO_3	—	76 ± 3	-1.4 V vs. SCE	[117]
Cu-Pt bimetallic	12.5 mM Na_2SO_4, 30 mg L^{-1} NO_3^-	194.4 ± 3.6 mg $g_{cat.}^{-1}$ L^{-1}	22	-0.4 V vs. RHE	[118]
Cu_xNi_y/NC	0.5 M Na_2SO_4, 50 mg L^{-1} NO_3^-	133 μg h^{-1} cm^{-2}	~50	-0.67 V vs. SCE	[119]
CuFe	0.1 M K_2SO_4, 2 mM KNO_3	0.23 mmol h^{-1} cm^{-2}	94.5	-0.7 V vs. RHE	[120]
Cu/rGO/GP	0.02 M NaCl, 0.02 M $NaNO_3$	203 μg h^{-1} cm^{-2}	—	-1.4 V vs. SCE	[121]
pCuO-10	0.05 M H_2SO_4, 0.05 M KNO_3	334 mmol cm^{-2} h^{-1}	—	-0.7 V vs. RHE	[122]
Cu (100), Cu (111)	0.1 M $HClO_4$, 2 mM $NaNO_3$	—	—	—	[61]
BDD/Cu film	0.1 mol L^{-1} Na_2SO_4, 0.1 mol L^{-1} KNO_3	—	—	—	[123]

to $NH_{(abs)}$ (0.23 eV) compared to the high activation energy of $NHOH_{(abs)}$ to $NH_2OH_{(abs)}$ (1.36 eV). The kinetic energy barrier and free energy analysis results confirm that Pathway D is the optimal reaction path.

$$NO_{(abs)} + H^+ + e^- \rightarrow NOH_{(abs)} \quad (12)$$

$$NOH_{(abs)} + H^+ + e^- \rightarrow NHOH_{(abs)} \quad (13)$$

$$NHOH_{(abs)} + H^+ + e^- \rightarrow NH_2OH_{(abs)} \quad (14)$$

$$NH_2OH_{(abs)} + H^+ + e^- \rightarrow NH_{2(abs)} + H_2O \quad (15)$$

$$NH_{2(abs)} + H^+ + e^- \rightarrow NH_{3(abs)} \quad (16)$$

$$NO_{(abs)} + 2H^+ + 2e^- \rightarrow N_{(abs)} + H_2O \quad (17)$$

$$N_{(abs)} + H^+ + e^- \rightarrow NH_{(abs)} \quad (18)$$

$$NH_{(abs)} + H^+ + e^- \rightarrow NH_{2(abs)} \quad (19)$$

$$NH_{2(abs)} + H^+ + e^- \rightarrow NH_{3(abs)} \quad (20)$$

$$NHOH_{(abs)} + H^+ + e^- \rightarrow NH_{(abs)} + H_2O \quad (21)$$

DOI: 10.14102/j.cnki.0254-5861.2022-0201

Table 2. Performance of Cu-Based Electrocatalysts for the Reduction of Nitrate to Ammonia under Alkaline Conditions.

electrocatalysts	electrolytes	NH_3 yield rate	FE (%)	potentials (vs. RHE)	ref.
Cu_6Sn_5-Sn NPs	1 M KOH, 0.1 M KNO_3	1 mmol mg^{-1} h^{-1}	90	0 V	[124]
Ru&Cu/Cu_2O	1 M KOH, 0.1 M KNO_3	—	95	0.1 V	[125]
CuCoSP on Cu foil	0.1 M KOH, 0.1 M NO_3^-	1.17 mmol h^{-1} cm^{-2}	90.6	-0.175	[126]
Cu_2O/Cu	1 M KOH, 250 mg L^{-1} NO_3^-	2.17 mg cm^{-2} h^{-1}	84.36	-0.25	[26]
$Cu_{10}Ce_{10}$	1 M KOH, 1400 mg L^{-1}	0.99 mmol h^{-1} cm^{-2}	98.43	-0.23 V	[52]
CuPd nanocubes	1 M KOH, 1 M KNO_3	6.25 mol/g_{cat}*h	92.5	-0.5 V, -0.6 V	[127]
Cu-N-C SAC	0.1M KOH, 0.1 M KNO_3	12.5 mol_{NH3} g^{-1}_{Cu} h^{-1}	84.7	-1.00 V	[128]
$Co_{0.5}Cu_{0.5}$	1 M KOH, 50 mM KNO_3	—	95	-0.03 V	[129]
Cu nanodisks	0.1 M KOH, 10 mM KNO_3	2.16 mg mg^{-1}_{cat} h^{-1}	81.1	-0.5 V	[130]
Au_1Cu SAAs	0.1 M KOH, 7.14 mM NO_3^-	555 μg h^{-1} cm^{-2}	98.7	-0.2 V	[131]
Ru-CuNW	1 M KOH, 2,000 mg L^{-1} NO_3^-	—	96	0.04 V	[132]
BCN@Cu	0.1 M KOH, 100 mM NO_3^-	435.6 mmol h^{-1} $mg_{cat.}^{-1}$	89.3	-0.5 V	[133]
BCN@Cu/CNT	0.1 M KOH, 100 mM KNO_3	172,226.5 μg h^{-1} $mg_{cat.}^{-1}$	95.32	-0.6 V	[134]
Cu@NF	1 M KOH, 200 mg L^{-1}	0.252 mmol h^{-1} cm^{-2}	96.6	0.23 V	[60]
oxide-derived Cu (OD-Cu)	1 M KOH, 100 mM KNO_3	1.1 mmol h^{-1} cm^{-2}	92	-0.15 V	[65]
HSCu-AGB@C	1 M KOH, 0.1 M NO_3^-	487.8 mmol g^{-1}_{cat} h^{-1}	94.2	-0.2 V	[135]
CuO_X	0.1 M KOH, 50 mg L^{-1} NO_3^-	449.41 ± 12.18 μg h^{-1} mg_{cat}^{-1}	74.18 ± 2.27	-0.25 V	[136]
Cu@C	1 M KOH, 1 × 10^{-3} M NO_3^-	469.5 μg h^{-1} cm^{-2}	72.0	-0.9 V	[137]
Cu-NBs-100	1 M KOH, 0.1 M NO_3^-	650 mmol g_{cat}^{-1} h^{-1}	95.3	-0.15 V	[138]
BCN-Cu	0.1 M KOH, 100 mM NO_3^-	1900.07 μg h^{-1} cm^{-2}	98.23	-0.5 V	[139]
Cu nanosheets	0.1 M KOH, 10 mM KNO_3	390.1 μg mg_{Cu}^{-1} h^{-1}	99.7	-0.15 V	[140]
$Cu_{50}Ni_{50}$ alloy	1 M KOH, 0.1 M KNO_3		99	-0.15 V	[55]

n DEVELOPMENT OF COPPER-BASED ELECTROCATALYSTS FOR NO_3RR

Cu-based materials show great advantages in promoting selective electroreduction of nitrate to ammonia in neutral, acidic and alkaline conditions, in terms of high ammonia yield rate and FE, as summarized in Tables 1-2. In this section, we will discuss four typical kinds of Cu-based materials based on differences in compositional and structural design, including monometallic Cu catalysts, bimetallic Cu-based catalysts, Cu-based compounds, and Cu-based inorganic-organic hybrid materials and their derivatives in detail, with emphasis on their structural and compositional features and functional mechanisms in promoting nitrate-to-ammonia conversion.

Monometallic Cu Catalysts. Bulk metallic Cu shows potential for electrocatalytic nitrate reduction, however, suffers from several limitations including insufficient reactive sites on the surface and low intrinsic reactivity of reactive sites. Aiming to solve these mentioned limitations, more efforts have been devoted to finely tuning the morphology and structure of metallic Cu catalysts. Particularly, metallic Cu with various nanostructured morphologies have been developed and demonstrated enhanced electrocatalytic nitrate-to-ammonia capability. The synthesis of nanostructured metallic Cu often entails the reduction of Cu(I) or Cu(II) sources by means of synthetic techniques such as chemical treatment, electrochemical synthesis, photochemical techniques, sonochemical methods, and thermal treatment. The rational choice of synthetic technique is important to design nanostructured metallic Cu catalysts with desired shape, size, and morphology for various specific applications.

Two-dimensional nanostructures (e.g., nanosheets, nanoplates, nanoflakes) show great application prospect in the field of catalysis due to their structural features and fascinating physicochemical properties. As an example, Kang and co-workers utilized Cu nanosheets to catalyze the electroreduction of nitrate to ammonia.[140] In this study, {111}-exposing Cu nanosheets were prepared by solution-phase-synthesis, where ascorbic acid (AA) serving as reducing agent, and hexamethylenetetramine (HMTA) and tetradecyltrimethylammonium bromide (TTAB) as stabilizers (Figure 4a, b). Compared with Cu nanocubes and irregular Cu nanoparticles, competitive HER was suppressed to a greater extent on the {111}-exposing Cu nanosheets, and the reaction rate of the rate-determining step ($NO_3^- + H_2O + 2e \rightarrow NO_2^- + 2OH^-$) was largely enhanced. Under optimal conditions, the {111}-exposing Cu nanosheets could derive a NH_3 yield rate of 390.1 μg mg^{-1}_{Cu} h^{-1} with a NH_3 FE of 99.7% (Figure 4c).

Surface defect engineering serves as an effective means to tune the electrocatalytic properties of 2D Cu nanostructures through tailoring the local surface microstructure and electronic structure. For instance, Xu et al. reported CuO nanoplates (CuO NPs) could be converted into defect-rich Cu nanoplates (*dr*-Cu NPs) by in situ electroreduction (Figure 4d-f).[103] The enrichment of atomic defects in the converted *dr*-Cu NPs could promote the adsorption of nitrate ions and related intermediates on the electrocatalyst surface and inhibit the occurrence of side reactions, thus selectively promoting the NH_3 formation reaction pathway and achieving a significant NH_3 production rate of 781.25 μg h^{-1} mg^{-1} and NH_3 FE of 85.47% (Figure 4g). Another study by Liu group showed that Cu oxide catalysts could be reduced to metallic Cu with abundant stacking faults under the negative potential of NO_3RR.[87] The oxide-derived Cu was

DOI: 10.14102/j.cnki.0254-5861.2022-0201

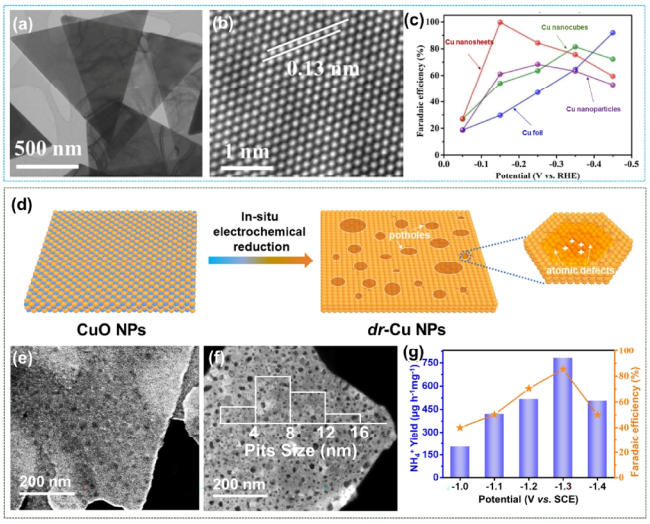

Figure 4. (a) Transmission electron microscopy (TEM) image of Cu nanosheets. (b) High resolution TEM (HRTEM) image of Cu nanosheets basal plane. (c) NH_3 FE of various Cu catalysts at different applied potentials. Reproduced with permission from Ref.[140] Copyright 2020, Elsevier. (d) Schematic illustration of the synthetic process, (e) scanning electron microscopy (SEM) image, (f) high-angle annular dark-field scanning TEM (HAADF- STEM) image, and (g) NH_3 yield rate and FE at different applied potentials for the *dr*-Cu NPs. Reproduced with permission from Ref.[103] Copyright 2021, Royal Society of Chemistry.

demonstrated as the actual active species for NO_3RR electrolysis and tensile strain effect was caused due to the in situ generated stacking faults. The features made the oxide-derived Cu more favorable for nitrate adsorption and largely enhance its nitrate-to-ammonia capability.

Dendritic nanostructures are another kind of promising and desirable electrode materials in electrocatalytic reactions. Compared with other nanostructures, dendritic nanostructures possess abundant catalytically active atoms at the edge and corner, which can function as catalytic sites and/or absorption sites for reactant molecules. In a study by Wang and co-workers, they constructed Cu nanodendrites (Cu NDs) grown along with the {200} facet by an electrodeposition method (Figure 5a).[95] Calculations by DFT in this study revealed that the reduction and protonation of nitrate on all faces of Cu proceeded spontaneously, with the disintegration of *NO intermediate being the rate-determining step (Figure 5b). From both experimental and theoretical results, it was demonstrated that electrocatalytic NO_3RR on Cu nanocatalysts was a facet-dependent process and Cu{200} offered lower activation energy for the dissociation of *NO intermediate (Figure 5c). The typical Cu NDs with {200} crystallographic planes exhibited outstanding electrochemical NO_3RR activity and achieved a high FE of 97%, using a $^{15}NO_3^-$ isotope labeling method to identify the source of generated NH_3. Hierarchical metallic Cu hollow nanostructures composed of 1D or 2D building blocks are also reported as efficient electrode materials to catalyze the NO_3RR. High-energy surfaces in these 1D or 2D building blocks could bring about more exposed active sites. A two-step conversion strategy was developed by Li et al. to fabricate hierarchical Cu nanosheet-based nanotubes (Cu NTs) by using pre-synthesized Cu nanowires (Cu NWs) as the starting material (Figure 5d).[141] Cu NWs were first chemically oxidized by H_2O_2 into CuO nanotubes (Figure 5e), which were then in-situ electrochemically reduced into Cu NTs (Figure 5f) under NO_3RR operating conditions. Cu NWs to Cu NTs conversion could expose more catalytically active sites and accelerate the charge and mass transfer in electrocatalysis, thus boosting electrocatalytic nitrate-to-ammonia capability. At -1.3 V (vs. saturated calomel electrode, SCE), Cu NTs could achieve 778.6 μg h^{-1} mg^{-1} of NH_3 yield, and 85.7% of FE NH_3 (Figure 5g).

Cu-Based Bimetallic Catalysts. Cu-based bimetallic catalysts as a new set of catalysts are prepared by mixing Cu and another kind of metal component within a single catalyst. It is well recognized that the bimetallic effect endows Cu-based bimetallic catalysts with unique electronic and chemical properties, which makes the properties of Cu-based bimetallic catalysts significantly different from monometallic Cu counterpart and offers opportunities to construct new catalysts with enhanced performance towards specific reactions.

One common strategy to construct Cu-based bimetallic catalysts is decorating preformed Cu nanostructures with another foreign metal component. The weak adsorption of H on Cu surface is recognized as the main limiting actor for ammonia synthesis from nitrate electroreduction on bare Cu surface. Aiming to enhance the hydrogenation capability of bare Cu, Luo and co-workers developed Cu nanowires (Cu NWs) coated with Rh single-atom (Rh@Cu) by galvanic replacement reaction

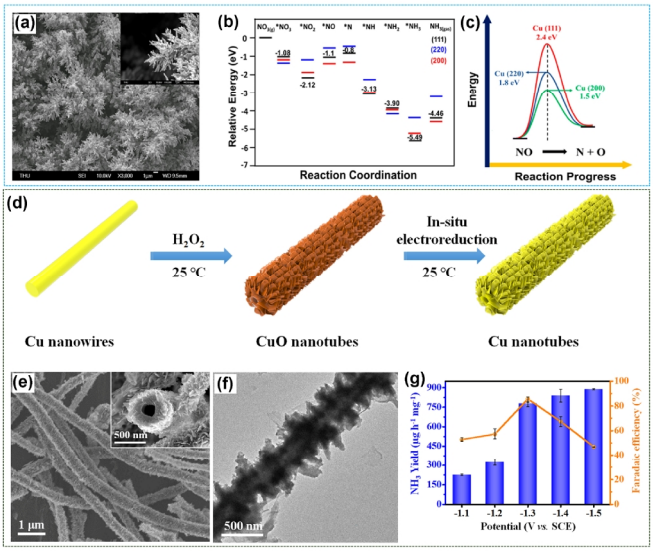

Figure 5. (a) SEM images of Cu NDs. (b) Potential energy diagram of NO_3RR on Cu{200}, Cu{220}, and Cu{111} surfaces. (c) Energy profile of NO dissociation on Cu{200}, Cu{220}, and Cu{111} surfaces. Reproduced with permission from Ref.[95] Copyright 2021, America Chemical Society. (d) Schematic illustration of the synthetic process of Cu nanotubes. (e) SEM image of CuO nanotubes, (f) TEM image of Cu nanotubes. (g) NH_3 yield rate and FE at different applied potentials for Cu nanotubes. Reproduced with permission from Ref.[141] Copyright 2022, Royal Society of Chemistry.

DOI: 10.14102/j.cnki.0254-5861.2022-0201

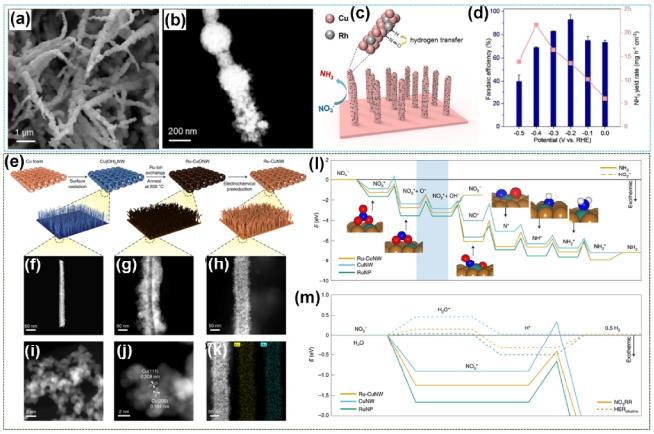

Figure 6. (a) SEM image, (b) HAADF-STEM image, (c) schematic illustration of the electrocatalytic NO_3RR process, (d) NH_3 yield rate and FE at different applied potentials for the Rh@Cu catalyst. Reproduced with permission from Ref.[91] Copyright 2022, WILEY-VCH. (e) Schematic illustration of the synthetic process of Ru-Cu NW. HAADF-STEM images of (f) $Cu(OH)_2$ NW, (g) Ru-CuO NW and (h) Ru-Cu NW. High-resolution HAADF-STEM images of (i) the Ru-CuNW surface structure and (j) its corresponding crystal structure and lattice spacing. (k) Energy-dispersive X-ray spectroscopy (EDS) mapping images of Ru-CuNW. (l) DFT-calculated minimum energy path for the NO_3RR. (m) Nitrate adsorption versus hydrogen evolution via an alkaline pathway on different catalytic surfaces. Reproduced with permission from Ref.[132] Copyright 2022, Nature Publishing Group.

between Cu and Rh^{3+} (Figure 6a,b).[91] Synergistic catalytic cooperation between Rh and Cu sites in the Rh@Cu catalyst could effectively accelerate surface hydrogenation rate during electrocatalytic NO_3RR process, as evidenced by the series of investigations including electron paramagnetic resonance, in situ infrared spectroscopy, differential electrochemical mass spectrometry and DFT modeling. Specifically, the Cu site in the Rh@Cu catalyst preferentially stabilized nitrogen intermediate species, whereas the vicinal Rh site could generate the activated H species, which were then transferred from Rh sites to the *NO-adsorbed intermediate species located on Cu sites, thus promoting the hydrogenation step for ammonia synthesis (Figure 6c). The highest NH_3 yield rate over the Rh@Cu catalyst could reach a record value of 1.27 mmol $h^{-1}cm^{-2}$ (Figure 6d). By a cation exchange method, Wang and colleague synthesized Ru-dispersed Cu nanowire catalyst (Ru-Cu NW) (Figure 6e-k).[132] Such a Ru-Cu NW catalyst could organically integrate the unique catalytic properties of Ru and Cu, that is, the highly dispersed Ru atoms could provide active nitrate reduction sites and the surrounding Cu sites could suppress the competitive HER. The combination of a suppressed HER, endothermic NO_2^- desorption and restricted movement of the N* species on the surface leads to a high NH_3 FE for Ru-Cu NW, as supported by DFT calculations (Figure 6l,m). When functioning as electrocatalysts for NO_3RR at NO_3^- concentrations of typical industrial wastewater (2,000 mg L^{-1}), the Ru-Cu NW could deliver an industrial-relevant NH_3 production rate of ~1 A cm^{-2} while maintaining a high NH_3 FE of 96%. With an over 99% nitrate conversion efficiency catalyzed by Ru-Cu NW catalyst, the nitrate concentration could be reduced from an industrial wastewater level to a drinkable water level.

Alloying Cu with another metal component to form bimetallic catalysts is another avenue to regulate their electronic structure and thus boost the electrocatalytic performance. In a study by Wang et al., they demonstrated enhanced nitrate-to-ammonia activity on CuNi alloys.[55] The composition of CuNi alloy system (e.g., Cu/Ni atomic ratio) had influence on the nitrate-to-ammonia activity. The optimal $Cu_{50}Ni_{50}$ alloy catalyst showed a 6-fold increase in nitrate-to-ammonia activity and a 0.2 V lower overpotential required to achieve the optimal NH_3 FE compared to pure Cu at 0 V vs. RHE (pH = 14). By investigating the electronic structure of catalysts using X-ray photoelectron spectroscopy (XPS), operando X-ray adsorption spectroscopy (XAS) and ultraviolet photoelectron spectroscopy (UPS), they found that the Cu d-band center upshifted toward the Fermi level in CuNi alloys and the adsorption energy of intermediates such as $*NO_3^-$, $*NO_2$ and $*NH_2$ could be regulated (Figure 7a). DFT simulations verified that alloying Cu with Ni moved the potential limiting step from NO_3^- adsorption to hydrogenation of $*NH_2$ intermediate due to the enhanced adsorption energy of NO_3^- on the CuNi surface and, thus lowering the overpotential (Figure 7b-d). In another example, mesoporous hollow sphere PdCu/Cu_2O hybrids containing highly dispersed PdCu alloys and an ultrathin Cu_2O shell showed high selectivity (96.70%) and FE

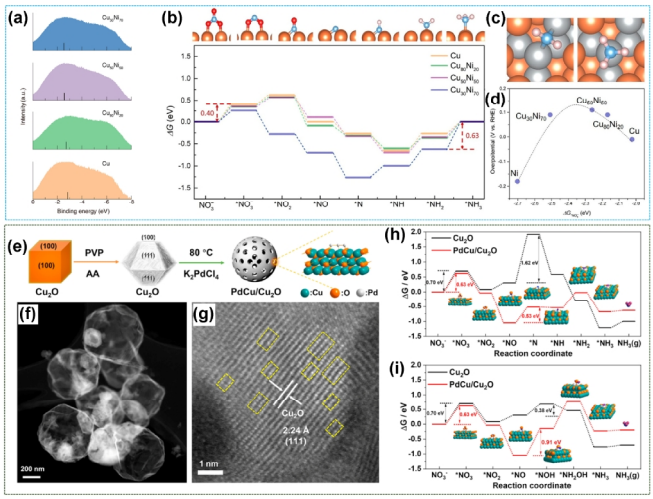

Figure 7. (a) UPS spectra and d-band center positions of pure Cu catalysts and the CuNi alloys. (b) Reaction free energies for different intermediates on a CuNi surface. (c) Hydrogenation reaction of $*NH_2$ on a $Cu_{30}Ni_{70}$ surface. (d) The volcano-type relationship between experimental overpotentials of NO_3RR at 5 mA cm^{-2} in 10 mM KNO_3 and adsorption energies of $*NO_3^-$ on all CuNi alloys. Reproduced with permission from Ref.[55] Copyright 2020, American Chemical Society. (e) Schematic illustration of the synthetic process of PdCu/Cu_2O hybrids. (f) Low-magnification HAADF-STEM image and (g) atomic-resolution HAADF-STEM image of PdCu/Cu_2O hybrids. (h, i) Reaction free energies for different intermediate during different NO_3RR paths. Reproduced with permission from Ref.[44] Copyright 2021, Elsevier B.V.

DOI: 10.14102/j.cnki.0254-5861.2022-0201

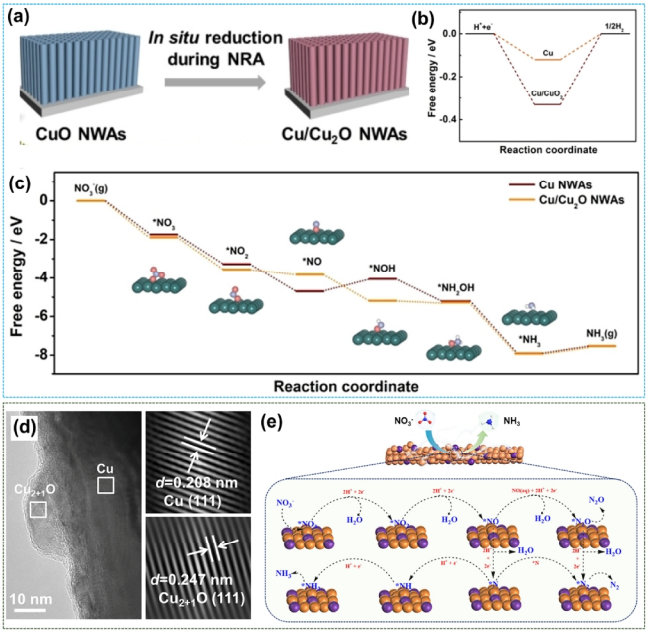

Figure 8. (a) Schematic illustration of the conversion process of Cu/Cu_2O NWAs from CuO NWAs. (b) The reaction energies of H_2 formation over Cu/Cu_2O NWAs and Cu NWAs. (c) Free energy diagram for NO_3RR over Cu NWAs and Cu/Cu_2O NWAs. Reproduced with permission from Ref.[98] Copyright 2020, WILEY-VCH. (d) HRTEM image of $Cu@Cu_{2+1}O$ NWs. (e) Schematic illustration showing the electrocatalytic nitrate reduction mechanism over the $Cu@Cu_{2+1}O$ NWs. Reproduced with permission from Ref.[100] Copyright 2021, Elsevier B.V.

(94.32%) for ammonia synthesis from nitrate (Figure 7e-g).[44] For this $PdCu/Cu_2O$ hybrid system, Pd enabled electron transfer from Pd 3d orbitals to Cu 3d orbitals and caused the polarization of Cu 3d orbitals by forming partial PdCu alloys. This feature made Pd electron deficient but offered empty orbitals to adsorb NO_3^-. The electron polarization effect also made electron-rich Cu more conducive to the occurrence of NO_3^- reduction. The combination of online differential electrochemical mass spectrometry and DFT calculations demonstrated that PdCu alloys block the generation of *NOH intermediate and facilitate the formation of *N (Figure 7h, i). Another example reported the construction of Au_1Cu (111) single-atom alloys with surface Cu vacancies (V_{Cu}-Au_1Cu SAAs) via a facile galvanic replacement with a subsequent dealloying process.[131] Single Au atoms and Cu vacancies worked synergistically on the neighboring Cu atoms, resulting in electron transfer from Cu site to Au site, which could promote the activation of H_2O to *H to boost NO_3^- hydrogenation kinetics and facilitate the desorption of $*NH_3$.

Cu-Based Compounds. Differing from monometallic or bimetallic Cu-based materials that contain Cu(0) species, Cu-based compounds usually possess Cu sites with oxidation states of +I or +II. Diverse chemical composition, morphology and electronic structure make Cu-based compounds potentially promising for catalyzing NO_3RR. Cu oxides, as the commonest Cu-based compounds, have been utilized in different areas of electrocatalysis. Recent investigations have further demonstrated their potential for electrochemical nitrate reduction. Zhang group reported the preparation of Cu/Cu_2O nanowire arrays (Cu/Cu_2O NWAs) as highly active catalysts for the electrochemical nitrate reduction to ammonia.[98] In this study, CuO NWAs were obtained by heat treatment of $Cu(OH)_2$ NWAs in an oxygen environment, which were then in situ converted to Cu/Cu_2O NWAs during the electrochemical process (Figure 8a). In-situ electrochemical reconstruction of the catalyst from CuO NWAs to Cu/Cu_2O NWAs was verified by in-situ electrochemical Raman spectroscopy, X-ray diffraction (XRD) patterns and auger electron spectroscopy (AES) spectroscopy. Electron transfer at the Cu/Cu_2O interface could regulate the electronic structure of converted Cu/Cu_2O NWAs and facilitate the formation of *NOH intermediate and suppress the competitive HER (Figure 8b, c), as confirmed by online differential electrochemical mass spectrometry (DEMS) and DFT calculation. Inspired by this work, Xu et al. developed a facile surface engineering strategy to fabricate Cu nanowires with concave-convex surface $Cu_{2+1}O$ layers ($Cu@Cu_{2+1}O$ NWs) (Figure 8d).[100] The electronic interaction and interface effect between $Cu/Cu_{2+1}O$ enabled tuning of the Cu d-band center and modulating the adsorption energies of intermediates, thus substantially enhancing the nitrate-to-ammonia capability (Figure 8e).

Incorporation of other appropriate metal with Cu oxides to form metal-Cu oxide composites can also enhance the performance of nitrate reduction to ammonia. Such metal-Cu oxide composites could function as dual-site or multi-site catalysts. The synergism of dual or multi active sites can potentially change the adsorption configuration of reactant molecules or intermediates, lower the energy barrier of key reaction steps and optimize the reaction path. Wang group constructed ultralow-content of Pd (2.93 at%) in-situ incorporated Cu_2O corner-etched octahedra composites (Pd-Cu_2O CEO) and demonstrated excellent nitrate conversion efficiency and ammonia yield.[107] It was found that a large number of cavities and oxygen vacancies were formed in the Pd-Cu_2O CEO composite during Pd introduction process. This synergistic effect of cavities and oxygen vacancy defects played a significant role in promoting nitrate adsorption, weakening the N-O bond and inhibiting by-product formation. In addition, Pd sites provided active centers for the accumulation of hydride species, which facilitated the reaction pathway for NH_3 formation. In another example, depositing Ag nanoparticles on Cu_2O with assistance of oxygen vacancies formed Ag/Cu_2O hybrids.[92] The formation of strong Ag-Cu bonds within Ag/Cu_2O hybrids could arouse strong interface interactions between Ag nanoparticles and Cu_2O. Moreover, the interface between Ag nanoparticles and Cu_2O was considered to function as new adsorption sites during NO_3RR electrocatalysis, which could efficiently boost the adsorption of NO_3^- and facilitate the formation of *N intermediates.

Coupling Cu-based oxides with other metal compounds to form heterostructured catalysts represents another strategy directed toward enhancing these catalytic systems. The presence of multiple constituents institutes a synergistic effect that endows the catalyst with superior performance and

DOI: 10.14102/j.cnki.0254-5861.2022-0201

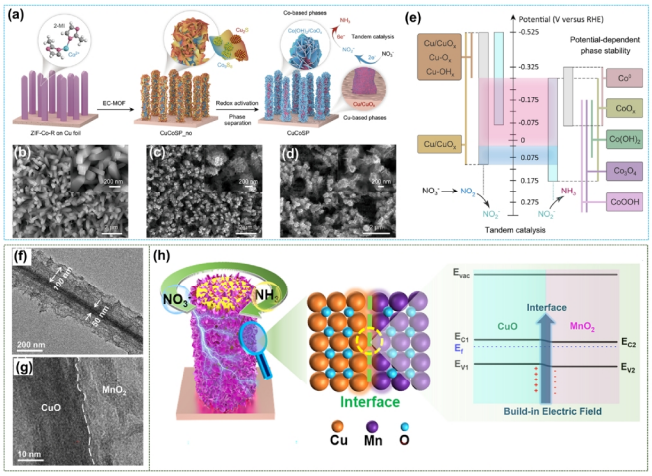

Figure 9. (a) Schematic illustration of the preparation of a Cu/Co-based binary tandem catalyst. SEM images of the (b) ZIF-Co-R precursor, (c) CuCoSP_no and (d) CuCoSP on the Cu foil substrate. (e) A proposed reaction mechanism of CuCoSP tandem catalysis of NO_3RR at low overpotentials. Reproduced with permission from Ref.[126] Copyright 2022, Nature Publishing Group. (f) TEM image and (g) HRTEM image of $CuO@MnO_2$ nanowires. (h) Schematic illustration showing schematic diagrams of the band structure of CuO and MnO_2, and the process of electrocatalytic nitrate reduction on the $CuO@MnO_2$/CF. Reproduced with permission from Ref.[101] Copyright 2022, Royal Society of Chemistry.

appreciable potential in a diverse range of catalytic applications. He et al. developed a tandem catalyst system for nitrate-to-ammonia conversion by electrochemical transformation of Cu-Co binary sulfide precursors into core-shell Cu/CuO_x and Co/CoO phases (Figure 9a-d).[126] It was found that the active Co^{2+}-based phases of CuCoSP were stabilized by the Cu/CuO_x phases, both of which were combined to form a tandem system for cascade nitrate-to-ammonia conversion at low overpotentials (Figure 9e). When functioning as electrocatalysts for NO_3RR, the inner Cu/CuO_x component preferentially catalyzed NO_3^- reduction to NO_2^-, which was rapidly reduced to NH_3 at the Co/CoO shell nearby, reaching a high NH_3 yield rate of 1.17 mmol cm^{-2} h^{-1} and a half-cell energy efficiency of ~36%. By covering 1D CuO nanowire arrays with 2D MnO_2 nanosheets, Xu et al. constructed hierarchical $CuO@MnO_2$ core-shell nanoarrays (Figure 9f, g).[101] Abundant exposed active sites and efficient mass transfer were obtained due to unique hierarchical core-shell nanoarray structures. More importantly, such a CuO/MnO_2 heterogeneous nanointerface could afford a well-designed built-in electric field at the interface region, which could trigger interfacial accumulation of nitrate ions and accelerate nitrate electroreduction kinetics by optimizing the chemisorption of nitrate ions or/and reaction intermediates (Figure 9h).

Apart from Cu oxides, other Cu-based compounds can also find potential applications in NO_3RR catalysis. Li and his colleagues reported that Cu_3P/CF composites were obtained by a simple in situ phosphorylation process as a promising binder-free electrode material for electrochemical NO_3RR.[142] They found that different phosphorylation temperatures had important effects on the catalytic activity and selectivity of the composites. As the phosphorylation temperature gradually increased, the nitrate conversion gradually decreased and reached the optimum conversion at 400 °C. Although the loading rate of Cu continued to increase when the temperature rose continually, the electron transfer efficiency and electrochemical activity area decreased, leading to a decrease in nitrate conversion. At the same time, ammonia selectivity continued to rise with increasing the phosphorylation temperature. At the optimal phosphorylation temperature (400 °C), the electrocatalytic nitrate reduction of the material achieved the best nitrate conversion (97.7%) with ammonia selectivity (~80%). It was observed that Cu_3P and Cu in copper foam play a dominant role in NO_3RR during the electrochemical process, rather than Cu^{2+} oxide species. These results suggested that suitable composition and crystallization, as well as high ECSA and interfacial electron transfer efficiency, were essential to ensure sufficient electrochemically active sites and superb electron transfer rates for electrocatalytic NO_3RR at the Cu_3P/CF composite electrode.

Cu-Based Inorganic-Organic Hybrid Materials and Their Derivatives. Inorganic-organic hybrid materials are a kind of functional materials composed of molecular or nanoscale inorganic and organic building blocks. For inorganic-organic hybrid materials, their properties not only depend on the kind and proportion, but also on their dispersion of individual constituents. In this section, we mainly focus on two kinds of Cu-based inorganic-organic hybrid materials for electrocatalytic NO_3RR application, that is, molecular catalysts and metal-organic frameworks (MOFs).

Molecular catalysts are promising in achieving high activity and selectivity in electrocatalytic nitrate-to-ammonia conversion due to the precise synthetic control. Moreover, molecular catalysts are also considered as appropriate platforms for gaining mechanistic insights into NO_3RR catalysis. Inspired by nitrate reductase, Wang and colleagues synthesized a Cu-based molecular solid catalyst by the incorporation of Cu in an organic molecular solid (3,4,9,10-perylenetetracarboxylic dianhydride, PTCDA) for eight-electron direct electroreduction of nitrate to ammonia.[47] Mechanism of performance improvement in the O-Cu-PTCDA (PTCDA with an optimum content of Cu) molecular solid catalyst was explanted from two aspects, supported by both electrochemical experiments and DFT calculations (Figure 10a-d). On one hand, the unique $3d^{10}$ configuration of Cu on PTCDA enabled Cu active center capable of effectively adsorbing NO_3^-, suppressing HER and boosting the H-N combination. On the other hand, the PTCDA structure facilitated the conduction of protons and electrons to the active Cu sites. These advantages endowed the O-Cu-PTCDA molecular solid catalyst with impressive capability for direct reduction of NO_3^- into NH_3 with a high selectivity.

MOF materials have great potential in electrocatalysis due to their structural specificity, uniformity, and designability. Unsaturated coordination environments with single metal sites have been shown to significantly enhance the catalytic activity of different reactions. MOF materials are promising carriers for the preparation of single-center catalysts. The Luo group modified

DOI: 10.14102/j.cnki.0254-5861.2022-0201

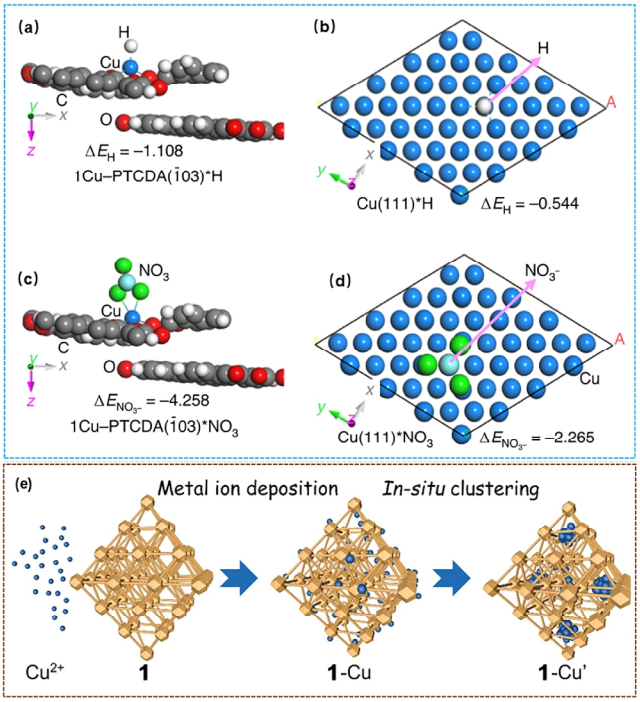

Figure 10. (a, c) The adsorption energies of H (a) and NO_3^- (c) on the surface of the O-Cu-PTCDA molecular layer (1̄03). (b, d) The adsorption energies of H (b) and NO_3^- (d) on the (111) plane of Cu. Reproduced with permission from Ref.[47] Copyright 2020, Nature Publishing Group. (e) Preparation and evolution of the host-guest Cu catalyst through metal ion deposition and in situ clustering routes. Reproduced with permission from Ref.[85] Copyright 2022, America Chemical Society.

crystalline Th-BPYDC (BPYDC = 2,2′-bipyridine-5,5′-dicarboxylic acid) by solid-liquid post-synthesis to synthesize robust Th-MOF-supported single-center Cu materials (Cu@Th-BPYDC) for nitrate electroreduction.[143] Notably, the Cu sites exhibited a novel square unsaturated coordination structure determined by single-crystal X-ray diffraction. It was found that the combination of Cu with BPYDC greatly enhanced the electrical conductivity of the material. In addition, Cu in Cu@Th-BPYDC showed unsaturated coordination with organic ligands, which enhanced the electrocatalytic activity of the material. Meanwhile, the Cu site in electrocatalyst showed a planar tetra-ligand configuration as the effective active site for catalytic nitrate reduction, thus exhibiting high dispersion and density, which made it easier for the active center to bind NO_3^- in solution to promote the electroreduction process. As expected, Cu@Th-BPYDC exhibited excellent NO_3^- electroreduction performance, producing NH_3 in high yield (225.3 μmol h^{-1} cm^{-2}) and FE (94.5%). Cao and co-workers reported an anticollapse MOF (Ce-UiO-66)-supported single-atom Cu precatalyst for electrocatalytic NO_3RR.[85] In situ XAS revealed the association of the formation of real catalytic sites with the in situ clustering of single-atom Cu, leading to uniform ultrasmall Cu nanoclusters (*ca.* 4 nm) without excessive aggregation by the confinement effect of the host framework (Figure 10f). The DFT calculation further confirmed the size effect and unique host-guest interaction of the catalyst in facilitating the NO_3^- activation and reaction energy decrease.

Beyond being directly employed as electrocatalysts for nitrate-to-ammonia conversion, MOF materials can also function as promising precatalysts or platforms for constructing advanced catalysts with desired compositions to achieve high electrocatalytic activities. Ren et al. reported the incorporation of Pd into HKUST-1 to form a kind of Pd-incorporated Cu-based MOF with p orous octahedral structure (CuPd-MOF) (Figure 11a).[99] When serving as precatalysts for NO_3RR electrocatalysis, the CuPd-MOFs were in-situ reconstituted to Cu/Pd/CuO_x multi-phase heterostructure with porous nanonetwork structure under nitrate electroreduction operating conditions (Figure 11b), which acted as the actual catalytic active material for NO_3RR electrocatalysis. Electronic interaction between Cu, Pd, and CuO_x components

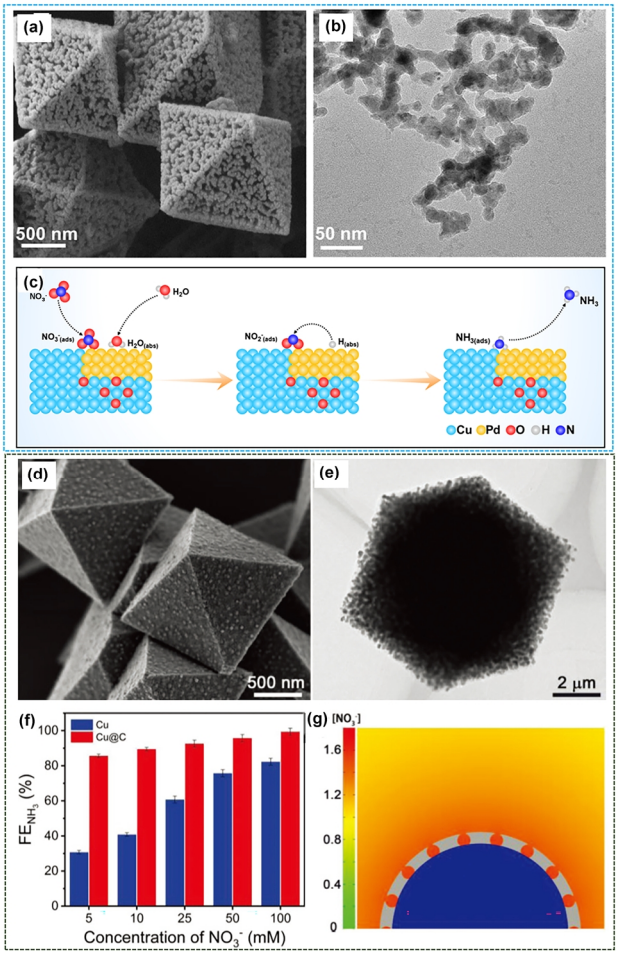

Figure 11. (a) SEM image of CuPd-MOF. (b) TEM image of Cu/Pd/CuO_x multi-phase heterostructure. (c) Schematic illustration showing the electrocatalytic nitrate-to-ammonia process over the Cu/Pd/CuO_x. Reproduced with permission from Ref.[99] Copyright 2022, Elsevier. (d) SEM image and (e) TME image of Cu@C catalyst. (f) Maximum FE NH_3 of Cu@C and Cu with concentrations of NO_3^- ranging from 5 to 100 × 10^{-3} M. (g) Simulated concentrations and distributions of local NO_3^- on the surface of Cu encapsulated with porous carbon. Reproduced with permission from Ref.[137] Copyright 2022, WILEY-VCH.

DOI: 10.14102/j.cnki.0254-5861.2022-0201

within the Cu/Pd/CuO_x multi-phase heterostructure could regulate the electronic structure of Pd sites and Cu sites. Electron transfer from Pd to Cu was demonstrated and electron-deficient feature for Pd sites could promote the NO_3^- adsorption on Pd sites, which was further reduced on electron-rich Cu sites (Figure 11c).

MOFs can be employed as precursors to prepare other functional materials through various pyrolytic, chemical, and physical treatments, and in combination with other types of materials. Cations in MOF structures are ideal source materials for various metals, metal oxides, and metal compounds, while the organic linkers provide the source materials for various pure and doped carbons. For most MOF-derived materials, they could inherit several of the desirable structural properties from MOFs, such as large surface areas and high levels of porosity, and could also be tailored to exhibit many new functionalities, either internally on their surfaces or a combination of both. These features endow MOF-derived functional materials with outstanding electrocatalytic properties. For example, Cu-BTC MOF with octahedral morphology was used as precursors for synthesizing Cu@C catalysts.[137] Conversion of Cu-BTC MOF into Cu@C material could be fulfilled by pyrolyzing the Cu-BTC MOF precursors at 700 °C in H_2 atmosphere, during which regular octahedral morphology was retained and Cu nanoparticles were in situ formed and encapsulated within the ligand-derived porous carbon framework (Figure 11d, e). One unique advantage in NO_3RR electrocatalysis for the Cu@C catalyst was its excellent nitrate-to-ammonia capability at ultralow NO_3^- concentrations. The enrichment effect of porous carbon framework in Cu@C structure was revealed to be the key factor that contributed to the enhancement in electrocatalytic performance as the presence of a porous carbon framework could effectively confine and concentrate NO_3^- on the surface of Cu@C catalyst and then facilitate the mass transfer of NO_3^- (Figure 11g). Compared with Cu nanoparticles (FE NH_3 of 19.9%), the Cu@C achieved a much higher FE NH_3 (72.0%) at -0.3 V vs. RHE in 1 × 10^{-3} M NO_3^-. Moreover, a wide tolerance range for concentration was demonstrated over the Cu@C catalysts, as the FE NH_3 of Cu@C exceeded 85.6% when the concentration of NO_3^- varied between 5 and 100 × 10^{-3} M (Figure 11f).

n CONCLUSION AND PERSPECTIVES

Electrochemical nitrate-to-ammonia conversion is considered as a technology of turning waste into wealth, which could remove environmentally harmful nitrate from various types of wastewaters while simultaneously producing value-added ammonia. Cu-based materials show great advantages in promoting selective electroreduction of nitrate to ammonia in terms of high nitrate conversion efficiency, NH_3 selectivity and NH_3 FE. A variety of Cu-based materials including monometallic Cu catalysts, bimetallic Cu-based catalysts, Cu-based compounds, and Cu-based inorganic-organic hybrid materials and their derivatives have been widely studied, and their merits have been explored in detail. With these material platforms, various strategies have been developed to tailored electronic structures of reactive sites by optimizing the morphology, structure, and composition of catalysts. Each type of Cu-based materials has its own advantages and disadvantages. Mono-

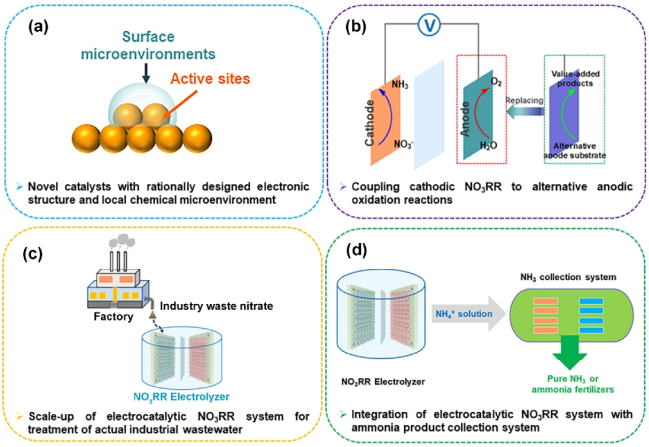

Figure 12. Prospects for developing NO_3RR technology for sustainable ammonia synthesis based on Cu-based materials.

metallic Cu catalysts are featured with simple composition and a single type of active site, which is convenient for studying their structure-activity relationships, while the weak adsorption of H on pure Cu surface is the main limiting factor for hydrogenation reaction during NO_3RR process. Bimetallic Cu-based catalysts can realize the regulation of electronic structure and properties of each metal to promote the adsorption and activation of reactants on the catalyst surface. Noted that many bimetallic Cu-based catalysts, like monometallic Cu, still face passivation or the leaching of metal species during NO_3RR catalysis process. As for Cu-based compounds, they possess diverse chemical composition, morphology and electronic structure. One of the main disadvantages for Cu-based compounds as cathodic catalysts lies in that they often undergo potential-dependent phase evolution under NO_3RR operating conditions, which make it become more difficult to elucidate and underlie catalytic mechanism. In the case of Cu-based inorganic-organic hybrid materials, their unique advantages include but not limited to high surface-to-volume ratio, intrinsically uniform metal site distribution, and structural tailorability. For most of them, insufficient electrical conductivity and low chemical stability under NO_3RR operating conditions are essential shortcomings. Moreover, current methods of synthesizing inorganic-organic hybrid materials are often high cost and difficult to be scaled up.

Although significant progress has been made, some problems and challenges need to be explored and resolved for Cu-based materials to electro-catalyze nitrate-to-ammonia conversion. First, inferior catalytic durability and stability are still the crucial issues that restrict the wider applications of Cu-based materials as most of them suffer from passivation (in alkaline conditions) or c orrosion and dissolution (in acidic environments). Second, the current ammonia yield rate and energy efficiency for nitrate-to-ammonia technology based on Cu-based materials are still far from the industrial requirements. Third, the separation and collection of ammonia product from aqueous-based electrocatalytic NO_3RR systems still face a double challenge from both technology and cost. To address these issues, great attention in

DOI: 10.14102/j.cnki.0254-5861.2022-0201

the future research should be paid to the following aspects:

Development of Novel Catalysts with Rationally Designed Electronic Structure and Local Chemical Microenvironment. Electrocatalysts play a dominant role in the nitrate-to-ammonia conversion process, as they largely affect the reaction efficiency. The activity and selectivity for electrocatalytic nitrate-to-ammonia conversion can be improved substantially through electronic structure regulation of catalysts to promote the adsorption and activation of nitrate and intermediates, and directionally change the reaction pathway. Current strategies for the design and construction of Cu-based catalysts mainly concentrate on modifying the electronic structure, increasing the active sites and enhancing the apparent or intrinsic activity of catalysts. Apart from the electronic structure of reactive sites of Cu-based catalysts, special attention should be paid to engineer the local chemical microenvironment of reactive sites including modulating the surface microenvironment of catalysts including their hydrophobicity, adsorbability, electronegativity and localization as these properties determine both the kinetic and thermodynamic catalytic processes (Figure 12a).

Innovation of Electrocatalytic NO_3RR System Based on Co-Electrolysis Mode. Energy conversion efficiency is one of the significant indicators of electrocatalytic NO_3RR system, as it is closely related to the final cost. For traditional aqueous-based electrocatalytic NO_3RR system, the major anodic reaction is the oxygen evolution reaction (OER). The sluggish kinetic of OER process generally results in a largely reduced overall electrolysis rate and energy conversion efficiency. Despite intensive efforts made to develop high-efficient OER catalysts for coupling with electrocatalytic NO_3RR, OER still suffers quite high oxidation potentials, leading to massive electric power consumption. Moreover, the product of anode OER is low-value oxygen. An innovative strategy is to rationally design anode reactions alternative to the traditional OER for the purpose of reducing power consumption and obtaining high value-added products (Figure 12b). In this regard, some recent advances have highlighted the promising potential to couple cathodic NO_3RR with the electrooxidation reaction of small organic molecules with value-added chemicals generated to lower the whole electrolysis voltage, elevate the NO_3RR performance and simultaneously generate value-added chemicals at anode. In addition to electrooxidation reaction of small organic molecules, more other anode reactions deserve more attention.

Scale-Up of Electrocatalytic NO_3RR System for Treatment of Actual Industrial Wastewater. As an attractive avenue to converting waste nitrate into value-added ammonia, NO_3RR electrocatalysis has recently received increasing attention with many papers have been published. However, most studies have focused on developing methods and strategies for catalyst preparation and few have been done in the way of large-scale demonstrations. In many published studies, manually prepared electrolytes containing nitrate addition rather than actual industrial wastewater are used in a lab test. For some electrocatalysts, the fluctuation and complexity of the actual water composition may cause performance delay in selective nitrate-to-ammonia conversion. Correspondingly, good thermal and chemical stability in the harsh conditions of real wastewater should be taken into account when designing electrocatalysts for NO_3RR (Figure 12c).

Integration of Electrocatalytic NO_3RR System with Ammonia Product Collection System. Another key obstacle for the development of nitrate-to-ammonia technology from basic re-search to practical applications lies in ammonia product collection. Current research in this field mainly concentrates on the nitrate-to-ammonia reaction, while isochronous NH_3 separation and recovery from the mother liquor are awfully neglected in state-of-the-art electrochemical NO_3RR systems. On one hand, ammonia product collection in forms of pure NH_3 or ammonia fertilizers (e.g., NH_4Cl, $(NH_4)_2SO_4$) is the prerequisite for its further utilization. On the other hand, the timely NH_3 separation can also promote the nitrate-to-ammonia conversion reaction due to the release of much more active sites. Gas stripping and membrane separation methods are potentially capable of ammonia recovery. Therefore, to promote the large-scale application of nitrate-to-ammonia technology, it is of great importance to electrochemically selective ammonia extraction from nitrate by integrating NO_3RR systems with NH_3 recovery system (Figure 12d).

n ACKNOWLEDGEMENTS

This work was financially supported by the National Natural Science Foundation of China (21701141).

n AUTHOR INFORMATION

Corresponding authors. Emails: 66246@bttc.edu.cn (L. W.) and yxu@zjut.edu.cn (Y. X.)

n COMPETING INTERESTS

The authors declare no competing interests.

n ADDITIONAL INFORMATION

Full paper can be accessed via
http://manu30.magtech.com.cn/jghx/EN/10.14102/j.cnki.0254-5861.2022-0201
For submission: https://www.editorialmanager.com/cjschem

n REFERENCES

(1) Yao, Y.; Zhu, S.; Wang, H.; Li, H.; Shao, M. A Spectroscopic study of electrochemical nitrogen and nitrate reduction on rhodium surfaces. *Angew. Chem., Int. Ed.* **2020**, 59, 10479-10483.

(2) Tang, C.; Qiao, S. Z. How to explore ambient electrocatalytic nitrogen reduction reliably and insightfully. *Chem. Soc. Rev.* **2019**, 48, 3166-3180.

(3) Qiu, W.; Xie, X.-Y.; Qiu, J.; Fang, W.-H.; Liang, R.; Ren, X.; Ji, X.; Cui, G.; Asiri, A. M.; Cui, G.; Tang, B.; Sun, X. High-performance artificial nitrogen fixation at ambient conditions using a metal-free electrocatalyst. *Nat. Commun.* **2018**, 9, 3485.

(4) Qu, Y.; Dai, T.; Cui, Y.; Zhang, Y.; Wang, Z.; Jiang, Q. Tailoring electronic structure of copper nanosheets by silver doping toward highly efficient electrochemical reduction of nitrogen to ammonia. *Chem. Eng. J.* **2022**, 433, 133752.

DOI: 10.14102/j.cnki.0254-5861.2022-0201

(5) Khalil, I. E.; Xue, C.; Liu, W.; Li, X.; Shen, Y.; Li, S.; Zhang, W.; Huo, F. The role of defects in metal-organic frameworks for nitrogen reduction reaction: when defects switch to features. *Adv. Funct. Mater.* **2021**, 31, 2010052.
(6) Ashida, Y.; Arashiba, K.; Nakajima, K.; Nishibayashi, Y. Molybdenum-catalysed ammonia production with samarium diiodide and alcohols or water. *Nature* **2019**, 568, 536-540.
(7) Wang, Y.; Yu, Y.; Jia, R.; Zhang, C.; Zhang, B. Electrochemical synthesis of nitric acid from air and ammonia through waste utilization. *Natl. Sci. Rev.* **2019**, 6, 730-738.
(8) Cui, X.; Tang, C.; Zhang, Q. A review of electrocatalytic reduction of dinitrogen to ammonia under ambient conditions. *Adv. Energy Mater.* **2018**, 8, 1800369.
(9) Utomo, W. P.; Leung, M. K. H.; Yin, Z.; Wu, H.; Ng, Y. H. Advancement of bismuth-based materials for electrocatalytic and photo(electro)catalytic ammonia synthesis. *Adv. Funct. Mater.* **2021**, 32, 2106713.
(10) Li, L.; Tang, C.; Yao, D.; Zheng, Y.; Qiao, S.-Z. Electrochemical nitrogen reduction: identification and elimination of contamination in electrolyte. *ACS Energy Lett.* **2019**, 4, 2111-2116.
(11) Liu, D.; Chen, M.; Du, X.; Ai, H.; Lo, K. H.; Wang, S.; Chen, S.; Xing, G.; Wang, X.; Pan, H. Development of electrocatalysts for efficient nitrogen reduction reaction under ambient condition. *Adv. Funct. Mater.* **2020**, 31, 2008983.
(12) Wan, Y.; Zhou, H.; Zheng, M.; Huang, Z. H.; Kang, F.; Li, J.; Lv, R. Oxidation state modulation of bismuth for efficient electrocatalytic nitrogen reduction to ammonia. *Adv. Funct. Mater.* **2021**, 31, 2100300.
(13) Tan, Y.; Yan, L.; Huang, C.; Zhang, W.; Qi, H.; Kang, L.; Pan, X.; Zhong, Y.; Hu, Y.; Ding, Y. Fabrication of an Au25-Cys-Mo electrocatalyst for efficient nitrogen reduction to ammonia under ambient conditions. *Small* **2021**, 17, 2100372.
(14) Hong, Q.; Li, T.; Zheng, S.; Chen, H.; Chu, H.; Xu, K.; Li, S.; Mei, Z.; Zhao, Q.; Ren, W. Tuning double layer structure of WO_3 nanobelt for promoting the electrochemical nitrogen reduction reaction in water. *Chin. J. Struct. Chem.* **2021**, 40, 519-526.
(15) Wang, G.; Shen, P.; Luo, Y.; Li, X.; Li, X.; Chu, K. A vacancy engineered MnO_{2-x} electrocatalyst promotes nitrate electroreduction to ammonia. *Dalton Trans.* **2022**, 51, 9206-9212.
(16) Xie, L.; Liu, Q.; Sun, S.; Hu, L.; Zhang, L.; Zhao, D.; Liu, Q.; Chen, J.; Li, J.; Ouyang, L.; Alshehri, A. A.; Hamdy, M. S.; Kong, Q.; Sun, X. High-efficiency electrosynthesis of ammonia with selective reduction of nitrate in neutral media enabled by self-supported Mn_2CoO_4 nanoarray. *ACS Appl. Mater. Interfaces* **2022**, 33242-33247.
(17) Niu, H.; Zhang, Z.; Wang, X.; Wan, X.; Shao, C.; Guo, Y. Theoretical insights into the mechanism of selective nitrate-to-ammonia electroreduction on single-atom catalysts. *Adv. Funct. Mater.* **2020**, 31, 2008533.
(18) Yan, L.; Xu, Z.; Liu, X.; Mahmood, S.; Shen, J.; Ning, J.; Li, S.; Zhong, Y.; Hu, Y. Integrating trifunctional Co@NC-CNTs@NiFe-LDH electrocatalysts with arrays of porous triangle carbon plates for high-power-density rechargeable Zn-air batteries and self-powered water splitting. *Chem. Eng. J.* **2022**, 446, 137049.
(19) Wang, S.; Wang, H.; Huang, C.; Ye, P.; Luo, X.; Ning, J.; Zhong, Y.; Hu, Y. Trifunctional electrocatalyst of N-doped graphitic carbon nanosheets encapsulated with CoFe alloy nanocrystals: the key roles of bimetal components and high-content graphitic-N. *Appl. Catal. B Environ.* **2021**, 298, 120512.
(20) Wu, Z. Y.; Karamad, M.; Yong, X.; Huang, Q.; Cullen, D. A.; Zhu, P.; Xia, C.; Xiao, Q.; Shakouri, M.; Chen, F. Y.; Kim, J. Y. T.; Xia, Y.; Heck, K.; Hu, Y.; Wong, M. S.; Li, Q.; Gates, I.; Siahrostami, S.; Wang, H. Electrochemical ammonia synthesis via nitrate reduction on Fe single atom catalyst. *Nat. Commun.* **2021**, 12, 2870.
(21) Chauhan, R.; Srivastava, V. C. Electrochemical denitrification of highly contaminated actual nitrate wastewater by Ti/RuO_2 anode and iron cathode. *Chem. Eng. J.* **2020**, 386, 122065.
(22) Li, J.; Zhang, Y.; Liu, C.; Zheng, L.; Petit, E.; Qi, K.; Zhang, Y.; Wu, H.; Wang, W.; Tiberj, A.; Wang, X.; Chhowalla, M.; Lajaunie, L.; Yu, R.; Voiry, D. 3.4% solar-to-ammonia efficiency from nitrate using Fe single atomic catalyst supported on MoS_2 nanosheets. *Adv. Funct. Mater.* **2021**, 32, 2108316.
(23) Lv, X.; Mou, T.; Li, J.; Kou, L.; Frauenheim, T. Tunable surface chemistry in heterogeneous bilayer single-atom catalysts for electrocatalytic NO_x reduction to ammonia. *Adv. Funct. Mater.* **2022**, 32, 2201262.
(24) Su, L.; Han, D.; Zhu, G.; Xu, H.; Luo, W.; Wang, L.; Jiang, W.; Dong, A.; Yang, J. Tailoring the assembly of iron nanoparticles in carbon microspheres toward high-performance electrocatalytic denitrification. *Nano Lett.* **2019**, 19, 5423-5430.
(25) Yu, H.; Qu, S.; Chen, P. R.; Ou, K. Q.; Lin, J. Y.; Guo, Z. H.; Zheng, L.; Li, J. K.; Huang, S.; Teng, Y.; Zou, L.; Song, J. L. CO_2 bubble-assisted in-situ construction of mesoporous Co-doped $Cu_2(OH)_2CO_3$ nanosheets as advanced electrodes towards fast and highly efficient electrochemical reduction of nitrate to N_2 in wastewater. *J. Hazard. Mater.* **2022**, 430, 128351.
(26) Fu, W.; Hu, Z.; Zheng, Y.; Su, P.; Zhang, Q.; Jiao, Y.; Zhou, M. Tuning mobility of intermediate and electron transfer to enhance electrochemical reduction of nitrate to ammonia on Cu_2O/Cu interface. *Chem. Eng. J.* **2022**, 433, 133680.
(27) Banasiak, L. J.; Schäfer, A. I. Removal of boron, fluoride and nitrate by electrodialysis in the presence of organic matter. *J. Membr. Sci.* **2009**, 334, 101-109.
(28) Samatya, S.; Kabay, N.; Yüksel, Ü.; Arda, M.; Yüksel, M. Removal of nitrate from aqueous solution by nitrate selective ion exchange resins. *React. Funct. Polym.* **2006**, 66, 1206-1214.
(29) Bae, B.-U.; Jung, Y.-H.; Han, W.-W.; Shin, H.-S. Improved brine recycling during nitrate removal using ion exchange. *Water Res.* **2002**, 36, 3330-3340.
(30) Xu, D.; Li, Y.; Yin, L.; Ji, Y.; Niu, J.; Yu, Y. Electrochemical removal of nitrate in industrial wastewater. *Front. Environ. Sci. Eng.* **2018**, 12, 9.
(31) Zhang, R.; Shuai, D.; Guy, K. A.; Shapley, J. R.; Strathmann, T. J.; Werth, C. J. Elucidation of nitrate reduction mechanisms on a Pd-In bimetallic catalyst using isotope labeled nitrogen species. *ChemCatChem* **2013**, 5, 313-321.
(32) Zhang, X.; Wang, Y.; Liu, C.; Yu, Y.; Lu, S.; Zhang, B. Recent advances in non-noble metal electrocatalysts for nitrate reduction. *Chem. Eng. J.* **2021**, 403, 126269.
(33) Clark, C. A.; Reddy, C. P.; Xu, H.; Heck, K. N.; Luo, G.; Senftle, T. P.; Wong, M. S. Mechanistic insights into pH-controlled nitrite reduction to ammonia and hydrazine over rhodium. *ACS Catal.* **2019**, 10, 494-509.
(34) Wei, L.; Liu, D.-J.; Rosales, B. A.; Evans, J. W.; Vela, J. Mild and selective hydrogenation of nitrate to ammonia in the absence of noble metals. *ACS Catal.* **2020**, 10, 3618-3628.

DOI: 10.14102/j.cnki.0254-5861.2022-0201

(35) Sun, W. J.; Ji, H. Q.; Li, L. X.; Zhang, H. Y.; Wang, Z. K.; He, J. H.; Lu, J. M. Built-in electric field triggered interfacial accumulation effect for efficient nitrate removal at ultra-low concentration and electroreduction to ammonia. *Angew. Chem., Int. Ed.* **2021**, 60, 22933-22939.

(36) Jia, R.; Wang, Y.; Wang, C.; Ling, Y.; Yu, Y.; Zhang, B. Boosting selective nitrate electroreduction to ammonium by constructing oxygen vacancies in TiO_2. *ACS Catal.* **2020**, 10, 3533-3540.

(37) Yu, Y.; Wang, C.; Yu, Y.; Wang, Y.; Zhang, B. Promoting selective electroreduction of nitrates to ammonia over electron-deficient Co modulated by rectifying Schottky contacts. *Sci. China: Chem.* **2020**, 63, 1469-1476.

(38) Li, Y.; Xiao, S.; Li, X.; Chang, C.; Xie, M.; Xu, J.; Yang, Z. A robust metal-free electrocatalyst for nitrate reduction reaction to synthesize ammonia. *Mater. Today Phys.* **2021**, 19, 100431.

(39) Kwon, Y.-I.; Kim, S. K.; Kim, Y. B.; Son, S. J.; Nam, G. D.; Park, H. J.; Cho, W.-C.; Yoon, H. C.; Joo, J. H. Nitric oxide utilization for ammonia production using solid electrolysis cell at atmospheric pressure. *ACS Energy Lett.* **2021**, 6, 4165-4172.

(40) Liang, J.; Liu, P.; Li, Q.; Li, T.; Yue, L.; Luo, Y.; Liu, Q.; Li, N.; Tang, B.; Alshehri, A. A.; Shakir, I.; Agboola, P. O.; Sun, C.; Sun, X. Amorphous boron carbide on titanium dioxide nanobelt arrays for high-efficiency electrocatalytic NO reduction to NH_3. *Angew. Chem., Int. Ed.* **2022**, 61, e202202087.

(41) Zhang, L.; Liang, J.; Wang, Y.; Mou, T.; Lin, Y.; Yue, L.; Li, T.; Liu, Q.; Luo, Y.; Li, N.; Tang, B.; Liu, Y.; Gao, S.; Alshehri, A. A.; Guo, X.; Ma, D.; Sun, X. High-performance electrochemical NO reduction into NH_3 by MoS_2 nanosheet. *Angew. Chem., Int. Ed.* **2021**, 60, 25263-25268.

(42) Ko, B. H.; Hasa, B.; Shin, H.; Zhao, Y.; Jiao, F. Electrochemical reduction of gaseous nitrogen oxides on transition metals at ambient conditions. *J. Am. Chem. Soc.* **2022**, 144, 1258-1266.

(43) Wang, Y.; Shu, S.; Peng, M.; Hu, L.; Lv, X.; Shen, Y.; Gong, H.; Jiang, G. Dual-site electrocatalytic nitrate reduction to ammonia on oxygen vacancy-enriched and Pd-decorated MnO_2 nanosheets. *Nanoscale* **2021**, 13, 17504-17511.

(44) Yin, H.; Chen, Z.; Xiong, S.; Chen, J.; Wang, C.; Wang, R.; Kuwahara, Y.; Luo, J.; Yamashita, H.; Peng, Y.; Li, J. Alloying effect-induced electron polarization drives nitrate electroreduction to ammonia. *Chem. Catal.* **2021**, 1, 1088-1103.

(45) Chen, Q.; Liang, J.; Yue, L.; Luo, Y.; Liu, Q.; Li, N.; Alshehri, A. A.; Li, T.; Guo, H.; Sun, X. CoO nanoparticle decorated N-doped carbon nanotubes: a high-efficiency catalyst for nitrate reduction to ammonia. *Chem. Commun.* **2022**, 58, 5901-5904.

(46) Fan, X.; Xie, L.; Liang, J.; Ren, Y.; Zhang, L.; Yue, L.; Li, T.; Luo, Y.; Li, N.; Tang, B.; Liu, Y.; Gao, S.; Alshehri, A. A.; Liu, Q.; Kong, Q.; Sun, X. In situ grown Fe_3O_4 particle on stainless steel: a highly efficient electrocatalyst for nitrate reduction to ammonia. *Nano Res.* **2021**, 15, 3050-3055.

(47) Chen, G.-F.; Yuan, Y.; Jiang, H.; Ren, S.-Y.; Ding, L.-X.; Ma, L.; Wu, T.; Lu, J.; Wang, H. Electrochemical reduction of nitrate to ammonia via direct eight-electron transfer using a copper-molecular solid catalyst. *Nat. Energy* **2020**, 5, 605-613.

(48) Crawford, J.; Yin, H.; Du, A.; O'Mullane, A. P. Nitrate-to-ammonia conversion at an InSn-enriched liquid-metal electrode. *Angew. Chem., Int. Ed.* **2022**, 61, e202201604.

(49) Deng, X.; Yang, Y.; Wang, L.; Fu, X. Z.; Luo, J. L. Metallic Co nanoarray catalyzes selective NH_3 production from electrochemical nitrate reduction at current densities exceeding 2 A cm^{-2}. *Adv. Sci.* **2021**, 8, 2004523.

(50) McEnaney, J. M.; Blair, S. J.; Nielander, A. C.; Schwalbe, J. A.; Koshy, D. M.; Cargnello, M.; Jaramillo, T. F. Electrolyte engineering for efficient electrochemical nitrate reduction to ammonia on a titanium electrode. *ACS Sustainable Chem. Eng.* **2020**, 8, 2672-2681.

(51) Li, Z.; Liang, J.; Liu, Q.; Xie, L.; Zhang, L.; Ren, Y.; Yue, L.; Li, N.; Tang, B.; Alshehri, A. A.; Hamdy, M. S.; Luo, Y.; Kong, Q.; Sun, X. High-efficiency ammonia electrosynthesis via selective reduction of nitrate on $ZnCo_2O_4$ nanosheet array. *Mater. Today Phys.* **2022**, 23, 100619.

(52) Yang, L.; Li, J.; Du, F.; Gao, J.; Liu, H.; Huang, S.; Zhang, H.; Li, C.; Guo, C. Interface engineering cerium-doped copper nanocrystal for efficient electrochemical nitrate-to-ammonia production. *Electrochim. Acta* **2022**, 411, 140095.

(53) Li, J.; Zhan, G.; Yang, J.; Quan, F.; Mao, C.; Liu, Y.; Wang, B.; Lei, F.; Li, L.; Chan, A. W. M.; Xu, L.; Shi, Y.; Du, Y.; Hao, W.; Wong, P. K.; Wang, J.; Dou, S. X.; Zhang, L.; Yu, J. C. Efficient ammonia electrosynthesis from nitrate on strained ruthenium nanoclusters. *J. Am. Chem. Soc.* **2020**, 142, 7036-7046.

(54) Lim, J.; Liu, C.-Y.; Park, J.; Liu, Y.-H.; Senftle, T. P.; Lee, S. W.; Hatzell, M. C. Structure sensitivity of Pd facets for enhanced electrochemical nitrate reduction to ammonia. *ACS Catal.* **2021**, 11, 7568-7577.

(55) Wang, Y.; Xu, A.; Wang, Z.; Huang, L.; Li, J.; Li, F.; Wicks, J.; Luo, M.; Nam, D. H.; Tan, C. S.; Ding, Y.; Wu, J.; Lum, Y.; Dinh, C. T.; Sinton, D.; Zheng, G.; Sargent, E. H. Enhanced nitrate-to-ammonia activity on copper-nickel alloys via tuning of intermediate adsorption. *J. Am. Chem. Soc.* **2020**, 142, 5702-5708.

(56) Wang, Z.; Young, S. D.; Goldsmith, B. R.; Singh, N. Increasing electrocatalytic nitrate reduction activity by controlling adsorption through PtRu alloying. *J. Catal.* **2021**, 395, 143-154.

(57) Zhu, J. Y.; Xue, Q.; Xue, Y. Y.; Ding, Y.; Li, F. M.; Jin, P.; Chen, P.; Chen, Y. Iridium nanotubes as bifunctional electrocatalysts for oxygen evolution and nitrate reduction reactions. *ACS Appl. Mater. Interfaces* **2020**, 12, 14064-14070.

(58) Yao, Q.; Chen, J.; Xiao, S.; Zhang, Y.; Zhou, X. Selective electrocatalytic reduction of nitrate to ammonia with nickel phosphide. *ACS Appl. Mater. Interfaces* **2021**, 13, 30458-30467.

(59) Wang, X.; Zhu, M.; Zeng, G.; Liu, X.; Fang, C.; Li, C. A three-dimensional Cu nanobelt cathode for highly efficient electrocatalytic nitrate reduction. *Nanoscale* **2020**, 12, 9385-9391.

(60) Li, J.; Gao, J.; Feng, T.; Zhang, H.; Liu, D.; Zhang, C.; Huang, S.; Wang, C.; Du, F.; Li, C.; Guo, C. Effect of supporting matrixes on performance of copper catalysts in electrochemical nitrate reduction to ammonia. *J. Power Sources* **2021**, 511, 230463.

(61) Pérez-Gallent, E.; Figueiredo, M. C.; Katsounaros, I.; Koper, M. T. M. Electrocatalytic reduction of nitrate on copper single crystals in acidic and alkaline solutions. *Electrochim. Acta* **2017**, 227, 77-84.

(62) Li, L.-X.; Sun, W.-J.; Zhang, H.-Y.; Wei, J.-L.; Wang, S.-X.; He, J.-H.; Li, N.-J.; Xu, Q.-F.; Chen, D.-Y.; Li, H.; Lu, J.-M. Highly efficient and selective nitrate electroreduction to ammonia catalyzed by molecular copper catalyst@$Ti_3C_2T_x$ MXene. *J. Mater. Chem. A* **2021**, 9, 21771-21778.

(63) Wang, Z.; Richards, D.; Singh, N. Recent discoveries in the reaction mechanism of heterogeneous electrocatalytic nitrate reduction. *Catal. Sci. Technol.* **2021**, 11, 705-725.

(64) Bae, S.-E.; Stewart, K. L.; Gewirth, A. A. Nitrate adsorption and

DOI: 10.14102/j.cnki.0254-5861.2022-0201

reduction on Cu(100) in acidic solution. *J. Am. Chem. Soc.* **2007**, 129, 10171-10180.

(65) Yuan, J.; Xing, Z.; Tang, Y.; Liu, C. Tuning the oxidation state of Cu electrodes for selective electrosynthesis of ammonia from nitrate. *ACS Appl. Mater. Interfaces* **2021**, 52469-52478.

(66) Gao, J.; Jiang, B.; Ni, C.; Qi, Y.; Zhang, Y.; Oturan, N.; Oturan, M. A. Non-precious Co_3O_4-TiO_2/Ti cathode based electrocatalytic nitrate reduction: preparation, performance and mechanism. *Appl. Catal. B Environ.* **2019**, 254, 391-402.

(67) Gao, J.; Jiang, B.; Ni, C.; Qi, Y.; Bi, X. Enhanced reduction of nitrate by noble metal-free electrocatalysis on P doped three-dimensional Co_3O_4 cathode: mechanism exploration from both experimental and DFT studies. *Chem. Eng. J.* **2020**, 382, 123034.

(68) Liu, R.; Zhao, H.; Zhao, X.; He, Z.; Lai, Y.; Shan, W.; Bekana, D.; Li, G.; Liu, J. Defect sites in ultrathin Pd nanowires facilitate the highly efficient electrochemical hydrodechlorination of pollutants by H*ads. *Environ. Sci. Technol.* **2018**, 52, 9992-10002.

(69) Martínez, J.; Ortiz, A.; Ortiz, I. State-of-the-art and perspectives of the catalytic and electrocatalytic reduction of aqueous nitrates. *Appl. Catal. B Environ.* **2017**, 207, 42-59.

(70) de Vooys, A. C. A.; van Santen, R. A.; van Veen, J. A. R. Electrocatalytic reduction of NO_3^- on palladium/copper electrodes. *J. Mol. Catal. A: Chem.* **2000**, 154, 203-215.

(71) Wang, Y.; Wang, C.; Li, M.; Yu, Y.; Zhang, B. Nitrate electroreduction: mechanism insight, in situ characterization, performance evaluation, and challenges. *Chem. Soc. Rev.* **2021**, 50, 6720-6733.

(72) Garcia-Segura, S.; Lanzarini-Lopes, M.; Hristovski, K.; Westerhoff, P. Electrocatalytic reduction of nitrate: fundamentals to full-scale water treatment applications. *Appl. Catal. B Environ.* **2018**, 236, 546-568.

(73) Wang, J.; Feng, T.; Chen, J.; Ramalingam, V.; Li, Z.; Kabtamu, D. M.; He, J.-H.; Fang, X. Electrocatalytic nitrate/nitrite reduction to ammonia synthesis using metal nanocatalysts and bio-inspired metalloenzymes. *Nano Energy* **2021**, 86, 106088.

(74) Lu, X.; Song, H.; Cai, J.; Lu, S. Recent development of electrochemical nitrate reduction to ammonia: a mini review. *Electrochem. Commun.* **2021**, 129, 107094.

(75) Zeng, Y.; Priest, C.; Wang, G.; Wu, G. Restoring the nitrogen cycle by electrochemical reduction of nitrate: progress and prospects. *Small Methods* **2020**, 4, 2000672.

(76) Duca, M.; Koper, M. T. Powering denitrification: the perspectives of electrocatalytic nitrate reduction. *Energy Environ. Sci.* **2012**, 5, 9726-9742.

(77) Li, P.; Jin, Z.; Fang, Z.; Yu, G. A single-site iron catalyst with preoccupied active centers that achieves selective ammonia electrosynthesis from nitrate. *Energy Environ. Sci.* **2021**, 14, 3522-3531.

(78) Liu, J.-X.; Richards, D.; Singh, N.; Goldsmith, B. R. Activity and selectivity trends in electrocatalytic nitrate reduction on transition metals. *ACS Catal.* **2019**, 9, 7052-7064.

(79) Crawford, J.; Yin, H.; Du, A.; O'Mullane, A. P. Nitrate-to-ammonia conversion at an insn-enriched liquid-metal electrode. *Angew. Chem.* **2022**, e202201604.

(80) Shih, Y.-J.; Wu, Z.-L.; Huang, Y.-H.; Huang, C.-P. Electrochemical nitrate reduction as affected by the crystal morphology and facet of copper nanoparticles supported on nickel foam electrodes (Cu/Ni). *Chem. Eng. J.* **2020**, 383, 123157.

(81) Hu, T.; Wang, C.; Wang, M.; Li, C. M.; Guo, C. Theoretical insights into superior nitrate reduction to ammonia performance of copper catalysts. *ACS Catal.* **2021**, 11, 14417-14427.

(82) Zhu, X.; Huang, H.; Zhang, H.; Zhang, Y.; Shi, P.; Qu, K.; Cheng, S.-B.; Wang, A.-L.; Lu, Q. Filling mesopores of conductive metal-organic frameworks with Cu clusters for selective nitrate reduction to ammonia. *ACS Appl. Mater. Interfaces* **2022**, 14, 32176-32182.

(83) Gong, Z.; Zhong, W.; He, Z.; Jia, C.; Zhou, D.; Zhang, N.; Kang, X.; Chen, Y. Improving electrochemical nitrate reduction activity of layered perovskite oxide La_2CuO_4 via B-site doping. *Catal. Today* **2022**, 402, 259-265.

(84) Niu, Z.; Fan, S.; Li, X.; Wang, P.; Tadé, M. O.; Liu, S. Optimizing oxidation state of octahedral copper for boosting electroreduction nitrate to ammonia. *ACS Appl. Energy Mater.* **2022**, 5, 3339-3345.

(85) Xu, Y.-T.; Xie, M.-Y.; Zhong, H.; Cao, Y. In situ clustering of single-atom copper precatalysts in a metal-organic framework for efficient electrocatalytic nitrate-to-ammonia reduction. *ACS Catal.* **2022**, 12, 8698-8706.

(86) Qiu, W.; Chen, X.; Liu, Y.; Xiao, D.; Wang, P.; Li, R.; Liu, K.; Jin, Z.; Li, P. Confining intermediates within a catalytic nanoreactor facilitates nitrate-to-ammonia electrosynthesis. *Appl. Catal. B Environ.* **2022**, 315, 121548.

(87) Fang, L.; Wang, S.; Song, C.; Lu, S.; Yang, X.; Qi, X.; Liu, H. Boosting nitrate electroreduction to ammonia via in situ generated stacking faults in oxide-derived copper. *Chem. Eng. J.* **2022**, 446, 137341.

(88) Cai, J.; Wei, Y.; Cao, A.; Huang, J.; Jiang, Z.; Lu, S.; Zang, S.-Q. Electrocatalytic nitrate-to-ammonia conversion with ~100% faradaic efficiency via single-atom alloying. *Appl. Catal. B Environ.* **2022**, 316, 121683.

(89) Gong, Z.; Zhong, W.; He, Z.; Liu, Q.; Chen, H.; Zhou, D.; Zhang, N.; Kang, X.; Chen, Y. Regulating surface oxygen species on copper(I) oxides via plasma treatment for effective reduction of nitrate to ammonia. *Appl. Catal. B Environ.* **2022**, 305, 121021.

(90) Liu, Y.; Deng, B.; Li, K.; Wang, H.; Sun, Y.; Dong, F. Metal-organic framework derived carbon-supported bimetallic copper-nickel alloy electrocatalysts for highly selective nitrate reduction to ammonia. *J. Colloid Interface Sci.* **2022**, 614, 405-414.

(91) Liu, H.; Lang, X.; Zhu, C.; Timoshenko, J.; Ruscher, M.; Bai, L.; Guijarro, N.; Yin, H.; Peng, Y.; Li, J.; Liu, Z.; Wang, W.; Cuenya, B. R.; Luo, J. Efficient electrochemical nitrate reduction to ammonia with copper-supported rhodium cluster and single-atom catalysts. *Angew. Chem., Int. Ed.* **2022**, 61, e202202556.

(92) Yin, H.; Zhao, X.; Xiong, S.; Peng, Y.; Chen, Z.; Wang, R.; Wen, M.; Luo, J.; Yamashita, H.; Li, J. New insight on electroreduction of nitrate to ammonia driven by oxygen vacancies-induced strong interface interactions. *J. Catal.* **2022**, 406, 39-47.

(93) Wang, C.; Ye, F.; Shen, J.; Xue, K. H.; Zhu, Y.; Li, C. In situ loading of Cu_2O active sites on island-like copper for efficient electrochemical reduction of nitrate to ammonia. *ACS Appl. Mater. Interfaces* **2022**, 14, 6680-6688.

(94) Jiang, G.; Peng, M.; Hu, L.; Ouyang, J.; Lv, X.; Yang, Z.; Liang, X.; Liu, Y.; Liu, H. Electron-deficient $Cu^{\delta+}$ stabilized by interfacial Cu-O-Al bonding for accelerating electrocatalytic nitrate conversion. *Chem. Eng. J.* **2022**, 435, 134853.

(95) Patil, S. B.; Liu, T. R.; Chou, H. L.; Huang, Y. B.; Chang, C. C.; Chen, Y. C.; Lin, Y. S.; Li, H.; Lee, Y. C.; Chang, Y. J.; Lai, Y. H.; Wen, C. Y.; Wang, D. Y. Electrocatalytic Reduction of NO_3^- to ultrapure ammonia on

DOI: 10.14102/j.cnki.0254-5861.2022-0201

{200} facet dominant Cu nanodendrites with high conversion faradaic efficiency. *J. Phys. Chem. Lett.* **2021**, 12, 8121-8128.

(96) Chen, L.-F.; Xie, A.-Y.; Lou, Y.-Y.; Tian, N.; Zhou, Z.-Y.; Sun, S.-G. Electrochemical synthesis of tetrahexahedral Cu nanocrystals with high-index facets for efficient nitrate electroreduction. *J. Electroanal. Chem.* **2022**, 907, 116022.

(97) Zhao, Y.; Liu, Y.; Zhang, Z.; Mo, Z.; Wang, C.; Gao, S. Flower-like open-structured polycrystalline copper with synergistic multi-crystal plane for efficient electrocatalytic reduction of nitrate to ammonia. *Nano Energy* **2022**, 97, 107124.

(98) Wang, Y.; Zhou, W.; Jia, R.; Yu, Y.; Zhang, B. Unveiling the activity origin of a copper-based electrocatalyst for selective nitrate reduction to ammonia. *Angew. Chem., Int. Ed.* **2020**, 59, 5350-5354.

(99) Ren, T.; Yu, Z.; Yu, H.; Deng, K.; Wang, Z.; Li, X.; Wang, H.; Wang, L.; Xu, Y. Interfacial polarization in metal-organic framework reconstructed Cu/Pd/CuO_x multi-phase heterostructures for electrocatalytic nitrate reduction to ammonia. *Appl. Catal. B Environ.* **2022**, 318, 121805.

(100) Ren, T.; Ren, K.; Wang, M.; Liu, M.; Wang, Z.; Wang, H.; Li, X.; Wang, L.; Xu, Y. Concave-convex surface oxide layers over copper nanowires boost electrochemical nitrate-to-ammonia conversion. *Chem. Eng. J.* **2021**, 426, 130759.

(101) Xu, Y.; Sheng, Y.; Wang, M.; Ren, T.; Shi, K.; Wang, Z.; Li, X.; Wang, L.; Wang, H. Interface coupling induced built-in electric fields boost electrochemical nitrate reduction to ammonia over CuO@MnO_2 core-shell hierarchical nanoarrays. *J. Mater. Chem. A* **2022**, 10, 16883-16890.

(102) Xu, Y.; Shi, K.; Ren, T.; Yu, H.; Deng, K.; Wang, X.; Wang, Z.; Wang, H.; Wang, L. Electronic metal-support interaction triggering interfacial charge polarization over CuPd/N-Doped-C nanohybrids drives selectively electrocatalytic conversion of nitrate to ammonia. *Small* **2022**, 2203335.

(103) Xu, Y.; Wang, M.; Ren, K.; Ren, T.; Liu, M.; Wang, Z.; Li, X.; Wang, L.; Wang, H. Atomic defects in pothole-rich two-dimensional copper nanoplates triggering enhanced electrocatalytic selective nitrate-to-ammonia transformation. *J. Mater. Chem. A* **2021**, 9, 16411-16417.

(104) Xu, Y.; Ren, K.; Ren, T.; Wang, M.; Liu, M.; Wang, Z.; Li, X.; Wang, L.; Wang, H. Cooperativity of Cu and Pd active sites in CuPd aerogels enhances nitrate electroreduction to ammonia. *Chem. Commun.* **2021**, 57, 7525-7528.

(105) Tang, Z.; Bai, Z.; Li, X.; Ding, L.; Zhang, B.; Chang, X. Chloride-derived bimetallic Cu-Fe nanoparticles for high-selective nitrate-to-ammonia electrochemical catalysis. *Processes* **2022**, 10, 751.

(106) Li, Z.; Wang, L.; Cai, Y.; Zhang, J.-R.; Zhu, W. Electrochemically reconstructed copper-polypyrrole nanofiber network for remediating nitrate-containing water at neutral pH. *J. Hazard. Mater.* **2022**, 440, 129828.

(107) Xu, Y.; Ren, K.; Ren, T.; Wang, M.; Wang, Z.; Li, X.; Wang, L.; Wang, H. Ultralow-content Pd in-situ incorporation mediated hierarchical defects in corner-etched Cu_2O octahedra for enhanced electrocatalytic nitrate reduction to ammonia. *Appl. Catal. B Environ.* **2022**, 306, 121094.

(108) Chen, D.; Zhang, S.; Bu, X.; Zhang, R.; Quan, Q.; Lai, Z.; Wang, W.; Meng, Y.; Yin, D.; Yip, S.; Liu, C.; Zhi, C.; Ho, J. C. Synergistic modulation of local environment for electrochemical nitrate reduction via asymmetric vacancies and adjacent ion clusters. *Nano Energy* **2022**, 98, 107338.

(109) Niu, Z.; Fan, S.; Li, X.; Liu, Z.; Wang, J.; Duan, J.; Tade, M. O.; Liu, S. Facile tailoring of the electronic structure and the d-band center of copper-doped cobaltate for efficient nitrate electrochemical hydrogenation. *ACS Appl. Mater. Interfaces* **2022**, 14, 35477-35484.

(110) Wang, J.; Zhang, S.; Wang, C.; Li, K.; Zha, Y.; Liu, M.; Zhang, H.; Shi, T. Ambient ammonia production via electrocatalytic nitrate reduction catalyzed by a flower-like $CuCo_2O_4$ electrocatalyst. *Inorg. Chem. Front.* **2022**, 9, 2374-2378.

(111) Zhu, T.; Chen, Q.; Liao, P.; Duan, W.; Liang, S.; Yan, Z.; Feng, C. Single-atom Cu catalysts for enhanced electrocatalytic nitrate reduction with significant alleviation of nitrite production. *Small* **2020**, 16, 2004526.

(112) Chen, Y.; Zhao, Y.; Zhao, Z.; Liu, Y. Highly dispersed face-centered cubic copper-cobalt alloys constructed by ultrafast carbothermal shock for efficient electrocatalytic nitrate-to-ammonia conversion. *Mater. Today Energy* **2022**, 29, 101112.

(113) Zhu, H.; Dong, S.; Du, X.; Du, H.; Xia, J.; Liu, Q.; Luo, Y.; Guo, H.; Li, T. Defective CuO-rich $CuFe_2O_4$ nanofibers enable the efficient synergistic electrochemical reduction of nitrate to ammonia. *Catal. Sci. Technol.* **2022**, 12, 4998-5002.

(114) Chen, H.; Zhang, C.; Sheng, L.; Wang, M.; Fu, W.; Gao, S.; Zhang, Z.; Chen, S.; Si, R.; Wang, L.; Yang, B. Copper single-atom catalyst as a high-performance electrocatalyst for nitrate-ammonium conversion. *J. Hazard. Mater.* **2022**, 434, 128892.

(115) Wang, H.; Guo, Y.; Li, C.; Yu, H.; Deng, K.; Wang, Z.; Li, X.; Xu, Y.; Wang, L. Cu/CuO_x in-plane heterostructured nanosheet arrays with rich oxygen vacancies enhance nitrate electroreduction to ammonia. *ACS Appl. Mater. Interfaces* **2022**, 14, 34761-34769.

(116) Xu, Y.; Wen, Y.; Ren, T.; Yu, H.; Deng, K.; Wang, Z.; Li, X.; Wang, L.; Wang, H. Engineering the surface chemical microenvironment over CuO nanowire arrays by polyaniline modification for efficient ammonia electrosynthesis from nitrate. *Appl. Catal. B Environ.* **2023**, 320, 121981.

(117) Hou, M.; Pu, Y.; Qi, W.-K.; Tang, Y.; Wan, P.; Yang, X. J.; Song, P.; Fisher, A. Enhanced electrocatalytic reduction of aqueous nitrate by modified copper catalyst through electrochemical deposition and annealing treatment. *Chem. Eng. Commun.* **2018**, 205, 706-715.

(118) Cerrón-Calle, G. A.; Fajardo, A. S.; Sánchez-Sánchez, C. M.; Garcia-Segura, S. Highly reactive Cu-Pt bimetallic 3D-electrocatalyst for selective nitrate reduction to ammonia. *Appl. Catal. B Environ.* **2022**, 302, 120844.

(119) Fang, L.; Wang, S.; Song, C.; Yang, X.; Li, Y.; Liu, H. Enhanced nitrate reduction reaction via efficient intermediate nitrite conversion on tunable Cu_xNi_y/NC electrocatalysts. *J. Hazard. Mater.* **2022**, 421, 126628.

(120) Wang, C.; Liu, Z.; Hu, T.; Li, J.; Dong, L.; Du, F.; Li, C.; Guo, C. Metasequoia-like nanocrystal of iron-doped copper for efficient electrocatalytic nitrate reduction into ammonia in neutral media. *ChemSusChem* **2021**, 14, 1825-1829.

(121) Yin, D.; Liu, Y.; Song, P.; Chen, P.; Liu, X.; Cai, L.; Zhang, L. In situ growth of copper/reduced graphene oxide on graphite surfaces for the electrocatalytic reduction of nitrate. *Electrochim. Acta* **2019**, 324, 134846.

(122) Daiyan, R.; Tran-Phu, T.; Kumar, P.; Iputera, K.; Tong, Z.; Leverett, J.; Khan, M. H. A.; Asghar Esmailpour, A.; Jalili, A.; Lim, M.; Tricoli, A.; Liu, R.-S.; Lu, X.; Lovell, E.; Amal, R. Nitrate reduction to ammonium: from CuO defect engineering to waste NO_x-to-NH_3 economic feasibility. *Energy Environ. Sci.* **2021**, 14, 3588-3598.

(123) Couto, A. B.; Santos, L. C. D.; Matsushima, J. T.; Baldan, M. R.; Ferreira, N. G. Hydrogen and oxygen plasma enhancement in the Cu electrodeposition and consolidation processes on BDD electrode applied to nitrate reduction. *Appl. Surf. Sci.* **2011**, 257, 10141-10146.

(124) Yu, J.; Kolln, A. F.; Jing, D.; Oh, J.; Liu, H.; Qi, Z.; Zhou, L.; Li, W.; Huang, W. Precisely controlled synthesis of hybrid intermetallic-metal

DOI: 10.14102/j.cnki.0254-5861.2022-0201

nanoparticles for nitrate electroreduction. *ACS Appl. Mater. Interfaces* **2021**, 13, 52073-52081.
(125) Cai, J.; Qin, S.; Akram, M. A.; Hou, X.; Jin, P.; Wang, F.; Zhu, B.; Li, X.; Feng, L. In situ reconstruction enhanced dual-site catalysis towards nitrate electroreduction to ammonia. *J. Mater. Chem. A* **2022**, 10, 12669-12678.
(126) He, W.; Zhang, J.; Dieckhofer, S.; Varhade, S.; Brix, A. C.; Lielpetere, A.; Seisel, S.; Junqueira, J. R. C.; Schuhmann, W. Splicing the active phases of copper/cobalt-based catalysts achieves high-rate tandem electroreduction of nitrate to ammonia. *Nat. Commun.* **2022**, 13, 1129.
(127) Gao, Q.; Pillai, H. S.; Huang, Y.; Liu, S.; Mu, Q.; Han, X.; Yan, Z.; Zhou, H.; He, Q.; Xin, H.; Zhu, H. Breaking adsorption-energy scaling limitations of electrocatalytic nitrate reduction on intermetallic CuPd nanocubes by machine-learned insights. *Nat. Commun.* **2022**, 13, 2338.
(128) Yang, J.; Qi, H.; Li, A.; Liu, X.; Yang, X.; Zhang, S.; Zhao, Q.; Jiang, Q.; Su, Y.; Zhang, L.; Li, J. F.; Tian, Z. Q.; Liu, W.; Wang, A.; Zhang, T. Potential-driven restructuring of Cu single atoms to nanoparticles for boosting the electrochemical reduction of nitrate to ammonia. *J. Am. Chem. Soc.* **2022**, 144, 12062-12071.
(129) Jeon, T. H.; Wu, Z.-Y.; Chen, F.-Y.; Choi, W.; Alvarez, P. J. J.; Wang, H. Cobalt-copper nanoparticles on three-dimensional substrate for efficient ammonia synthesis via electrocatalytic nitrate reduction. *J. Phys. Chem. C* **2022**, 126, 6982-6989.
(130) Wu, K.; Sun, C.; Wang, Z.; Song, Q.; Bai, X.; Yu, X.; Li, Q.; Wang, Z.; Zhang, H.; Zhang, J.; Tong, X.; Liang, Y.; Khosla, A.; Zhao, Z. Surface reconstruction on uniform Cu nanodisks boosted electrochemical nitrate reduction to ammonia. *ACS Mater. Lett.* **2022**, 4, 650-656.
(131) Zhang, Y.; Chen, X.; Wang, W.; Yin, L.; Crittenden, J. C. Electrocatalytic nitrate reduction to ammonia on defective Au1Cu (111) single-atom alloys. *Appl. Catal. B Environ.* **2022**, 310, 121346.
(132) Chen, F. Y.; Wu, Z. Y.; Gupta, S.; Rivera, D. J.; Lambeets, S. V.; Pecaut, S.; Kim, J. Y. T.; Zhu, P.; Finfrock, Y. Z.; Meira, D. M.; King, G.; Gao, G.; Xu, W.; Cullen, D. A.; Zhou, H.; Han, Y.; Perea, D. E.; Muhich, C. L.; Wang, H. Efficient conversion of low-concentration nitrate sources into ammonia on a Ru-dispersed Cu nanowire electrocatalyst. *Nat. Nanotechnol.* **2022**, 17, 759-767.
(133) Zhao, X.; Hu, G.; Tan, F.; Zhang, S.; Wang, X.; Hu, X.; Kuklin, A. V.; Baryshnikov, G. V.; Ågren, H.; Zhou, X.; Zhang, H. Copper confined in vesicle-like BCN cavities promotes electrochemical reduction of nitrate to ammonia in water. *J. Mater. Chem. A* **2021**, 9, 23675-23686.
(134) Zhao, X.; Li, X.; Zhang, H.; Chen, X.; Xu, J.; Yang, J.; Zhang, H.; Hu, G. Atomic-dispersed copper simultaneously achieve high-efficiency removal and high-value-added conversion to ammonia of nitrate in sewage. *J. Hazard. Mater.* **2022**, 424 (Pt A), 127319.
(135) Hu, Q.; Qin, Y.; Wang, X.; Zheng, H.; Gao, K.; Yang, H.; Zhang, P.; Shao, M.; He, C. Grain boundaries engineering of hollow copper nanoparticles enables highly efficient ammonia electrosynthesis from nitrate. *CCS Chem.* **2022**, 4, 2053-2064.
(136) Geng, J.; Ji, S.; Xu, H.; Zhao, C.; Zhang, S.; Zhang, H. Electrochemical reduction of nitrate to ammonia in a fluidized electrocatalysis system with oxygen vacancy-rich CuO_x nanoparticles. *Inorg. Chem. Front.* **2021**, 8, 5209-5213.
(137) Song, Z.; Liu, Y.; Zhong, Y.; Guo, Q.; Zeng, J.; Geng, Z. Efficient electroreduction of nitrate into ammonia at ultralow concentrations via an enrichment effect. *Adv. Mater.* **2022**, 34, 2204306.
(138) Hu, Q.; Qin, Y.; Wang, X.; Wang, Z.; Huang, X.; Zheng, H.; Gao, K.; Yang, H.; Zhang, P.; Shao, M.; He, C. Reaction intermediate-mediated electrocatalyst synthesis favors specified facet and defect exposure for efficient nitrate-ammonia conversion. *Energy Environ. Sci.* **2021**, 14, 4989-4997.
(139) Zhao, X.; Jia, X.; He, Y.; Zhang, H.; Zhou, X.; Zhang, H.; Zhang, S.; Dong, Y.; Hu, X.; Kuklin, A. V.; Baryshnikov, G. V.; Ågren, H.; Hu, G. Two-dimensional BCN matrix inlaid with single-atom-Cu driven electrochemical nitrate reduction reaction to achieve sustainable industrial-grade production of ammonia. *Appl. Mater. Today* **2021**, 25, 101206.
(140) Fu, X.; Zhao, X.; Hu, X.; He, K.; Yu, Y.; Li, T.; Tu, Q.; Qian, X.; Yue, Q.; Wasielewski, M. R.; Kang, Y. Alternative route for electrochemical ammonia synthesis by reduction of nitrate on copper nanosheets. *Appl. Mater. Today* **2020**, 19, 100620.
(141) Li, C.; Liu, S.; Xu, Y.; Ren, T.; Guo, Y.; Wang, Z.; Li, X.; Wang, L.; Wang, H. Controllable reconstruction of copper nanowires into nanotubes for efficient electrocatalytic nitrate conversion into ammonia. *Nanoscale* **2022**, 14, 12332-12338.
(142) Yao, F.; Jia, M.; Yang, Q.; Chen, F.; Zhong, Y.; Chen, S.; He, L.; Pi, Z.; Hou, K.; Wang, D.; Li, X. Highly selective electrochemical nitrate reduction using copper phosphide self-supported copper foam electrode: performance, mechanism, and application. *Water Res.* **2021**, 193, 116881.
(143) Gao, Z.; Lai, Y.; Tao, Y.; Xiao, L.; Zhang, L.; Luo, F. Constructing well-defined and robust Th-MOF-supported single-site copper for production and storage of ammonia from electroreduction of nitrate. *ACS Cent. Sci.* **2021**, 7, 1066-1072.

Received: September 25, 2022
Accepted: November 12, 2022
Published online: November 22, 2022
Published: December 2, 2022

DOI: 10.14102/j.cnki.0254-5861.2022-0201

Tianlun Ren received his master's degree from Zhejiang University of Technology in 2021. He is currently studying for his Ph.D. degree at Zhejiang University of Technology. His main research work is the design and construction of efficient metal-based electrocatalysts for the electrochemical synthesis of ammonia from nitrogen and nitrate.

Youwei Sheng received his bachelor's degree from Nanjing University Jinling College in 2020. He is currently studying for his master's degree at Zhejiang University of Technology. His main research work focuses on the design and construction of electrocatalysts and their applications in electrochemical ammonia synthesis and electrochemical reduction of CO_2.

Mingzhen Wang received his bachelor's degree from Hefei University in 2018 and master's degree from Zhejiang University in 2022. His current research interests include the controlled preparation and construction of non-noble metal-based electrocatalysts for electrocatalytic nitrate reduction for ammonia production.

Kaili Ren received her bachelor's degree from Xinyang Normal University in 2019 and her master's degree from Zhejiang University of Technology in 2022. During the master's degree, her main research work is electrolysis of water to produce hydrogen and electrochemical nitrate reduction to synthesize ammonia.

Lianlian Wang received her Ph.D. degree from Changchun Institute of Optics Fine Mechanics and Physics (CIOMP), Chinese Academy of Sciences in 2013, and then she became a lecturer at Department of Chemistry, Baotou Teachers' College. Her current research work is the design and construction of nano functional materials and the application in luminescent fields.

You Xu received his Ph.D. degree from Tianjin University (China) in 2014. He worked as a postdoctoral researcher at Nanyang Technological University (Singapore) in 2014-2017. Since 2017, he has been an Associate Professor at the College of Chemical Engineering, Zhejiang University of Technology (China). His research interests include the development of advanced nanomaterials and their hybrids for electrocatalytic applications.

Chin. J. Struct. Chem. **2022**, 41, 2212089-2212106
DOI: 10.14102/j.cnki.0254-5861.2022-0201